COMPUTED FOURIER SERIES REPRESENTATIONS OF THE INTERACTION POTENTIAL OF AN ARGON ATOM ON AN ARGON CRYSTAL SURFACE

by

PAULINA MARIA STOOP

Submitted in partial fulfilment of
the requirements for the degree

MAGISTER SCIENTIAE

In the Faculty of Science
University of Pretoria

April 1986

SAMEVATTING

BEREKENDE FOURIERREEKS-VOORSTELLINGS VAN DIE WISSELWERKINGS-POTENSIAAL VAN 'N ARGON ATOOM OP 'N ARGON KRISTALOPPERVLAK.

deur

Paulina Maria Stoop

Leier : Prof. J.A. Snyman

Eksterne eksaminator: Prof. C.A.B. Ball

Departement : Toegepaste Wiskunde

Verhandeling ingedien vir die graad Magister Scientiae.

Die soeke na 'n Fourierreeks-voorstelling vir die adatoom-oppervlak wisselwerkingspotensiaal by 'n kristaloppervlak is ongetwyfeld van die allergrootste belang. Betroubare inligting aangaande numeriese waardes vir die Fourierkoëffisiënte is 'n voorvereiste vir vordering met die oplossing van baie probleme in oppervlakfisika. Sulke probleme is byvoorbeeld, verstrooiing vanaf kristalvlakke, die berekening van die termodinamiese eienskappe van geadsorbeerde atome, fase-oorgange in geadsorbeerde lagies, asook epitaksie.

Die doel van hierdie studie was om die betrokke Fourierkoëffisiënte van die ewewigswisselwerkingspotensiaal $\phi_e(x,y)$ en van die ewewigshoogte

$z_{min}(x,y)$ van 'n argon atoom by 'n (001) argon kristaloppervlak te bepaal. 'n Lennard-Jones (6-12) potensiaal is gebruik. Die omvang van die berekeninge het die afknotting van die Fourierreeks genoodsaak.

Die vorm van die reeks vir $\phi_e(x,y)$, onderhewig aan die simmetrie eienskappe wat deur die substraat afgedwing word, is analities afgelei deur van 'n suiwer wiskundige benadering, asook van die meer fisiese benadering van die omgekeerde rooster formalisme gebruik te maak.

Daar is 'n rekenaarprogram geskryf om die *ewewigs*-wisselwerkingsenergie $\phi_e(x,y)$ by enige punt in 'n twee-dimensionale eenheidsel bokant die kristallyne substraat te bereken. Die afknotting van die kristal by 5a, is deur rekenbeperkings genoodsaak en geregverdig deur die feit dat die waarde van $\phi_e(x,y)$ by die oorsprong met minder as 0,3% verander indien die radius van 5a na 6a vermeerder word, waar a die roosterparameter is.

Alle berekeninge is uitgevoer deur 144 datapunte te gebruik; meer datapunte het weinig bygedra om die akkuraatheid te verhoog. Die insluiting van hoër orde harmonieke het die waardes wat vir die laer orde koëffisiënte verkry is, nie wesenlik beïnvloed nie. Die Fourier koëffisiënte konvergeer vinnig na nul met harmoniese orde; die groottes van die vyfde orde koëffisiënte is slegs omtrent 0,04% van die eerste orde koëffisiënte.

Waardes vir die koëffisiënte in 'n een-dimensionale snit, wat verkry is deur $y = 0$ te stel in die twee-dimensionale voorstelling, is bevestig deur gebruik te maak van analitiese een-dimensionale uitdrukkings afgelei deur Hildebrand.

Die berekende desorpsie energie E_d en die oppervlakdiffusie aktiveringsenergie E_a van 'n geadsorbeerde atoom vergelyk goed met die wat deur Bacigalupi en Neustadter bereken is. E_d en E_a kan verkry word deur gebruik te maak van Fourier benaderings wat by lae ordes afgeknot is. Ten einde redelike resultate vir die waarde van die horisontale kragkonstante k_{xy} te verkry, moet ten minste derde orde harmonieke in die benadering ingesluit word.

Die koëffisiënte in die berekende Fourierreeks-voorstelling vir die ewewigshoogte konvergeer ook redelik vinnig na nul, alhoewel daar meer variasie in die groottes van die hoër orde koëffisiënte is. Dit kan moontlik aan numeriese afrondingsfoute toegeskryf word. Daar is aangetoon dat die ewewigshoogte by 'n adsorpsie posisie 0,52815a is wat 'n effense ontspanning van die (001) oppervlak verteenwoordig in ooreenstemming met vroeëre werk van L.C.A. Stoop.

SUMMARY

COMPUTED FOURIER SERIES REPRESENTATIONS OF THE INTERACTION POTENTIAL OF AN ARGON ATOM ON AN ARGON CRYSTAL SURFACE

by

Paulina Maria Stoop

Promotor : Prof. J.A. Snyman

External Examiner : Prof. C.A.B. Ball

Department : Applied Mathematics

Dissertation submitted for the degree Magister Scientiae.

Undoubtedly the quest for a Fourier series representation of the adatom-surface interaction potential at a crystal surface is of paramount importance. Reliable knowledge of the Fourier coefficients is a prerequisite for progress in the solution of many problems in surface physics. Such problems are for example, scattering from crystal surfaces, the evaluation of the thermodynamic properties of adsorbed atoms, phase transitions in adsorbed layers and epitaxy.

The purpose of this study was to calculate the relevant Fourier coefficients of the equilibrium interaction potential $\phi_e(x,y)$ and for the equilibrium height $z_{min}(x,y)$ of an argon atom above a (001) argon

crystal surface using a Lennard-Jones (6-12) potential. The extent of the numerical computations necessitated truncation of the Fourier series.

The form of the series for $\phi_e(x,y)$, subjected to the symmetry properties imposed by the substrate, was derived analytically using a purely mathematical approach and the more physical approach of the reciprocal lattice formalism.

A computer program was written to evaluate the *equilibrium* interaction energy $\phi_e(x,y)$ at any point in a two-dimensional unit cell above the crystal substrate. Truncation of the crystal at 5a (a being the lattice parameter) was also necessitated by computational limitations and was justified by the fact that increasing the radius from 5a to 6a altered $\phi_e(x,y)$ at the origin by less than 0,3%.

All calculations were carried out using 144 data points; using more data resulted in negligible increase of accuracy. Inclusion of higher order harmonics do not significantly influence the values obtained for the lower order coefficients. The Fourier coefficients converge rapidly to zero with harmonic order; the magnitudes of fifth order coefficients are only about 0,04% of those of the first order coefficients.

Values for coefficients in a one-dimensional section, obtained by putting $y = 0$ in the two-dimensional representation, were verified using analytical one-dimensional expressions derived by Hildebrand.

The calculated desorption energy E_d and the surface migration

activation energy E_a of an adsorbed atom compared well with those calculated by Bacigalupi and Neustadter. E_d and E_a can be obtained using Fourier approximations truncated at low orders. In order to obtain fair results for the value of the lateral force constant k_{xy}, at least third order harmonics must be included in the approximation.

The coefficients in the computed Fourier series representation of the equilibrium height also converge to zero fairly rapidly, but with more variance in the magnitudes of the higher order coefficients. This is possibly partly due to rounding off errors. It was shown that the equilibrium height at an adsorption site was 0,52815a which represents a slight outward relaxation of the (001) surface planes. This agrees well with previous work by L.C.A. Stoop.

CONTENTS

1. INTRODUCTION

In recent years surface physics has moved into the forefront of scientific progress. A great variety of processes of great scientific and technological interest, such as epitaxial growth, occur at surfaces and interfaces between materials. This progress was greatly stimulated by the development of sophisticated surface characterisation techniques, e.g. scanning tunneling microscopy [1]. This technique permits the observation of individual surface atoms and allows the resolution of both surface topography and electronic structure and is expected to contribute greatly to our understanding of surface phenomena [2].

The adatom-substrate interaction potential plays a decisive role in many surface processes. Some efforts have been directed towards the development of specifically designed surface interaction potentials. They are expected to be different from the atom-crystal potential in the bulk crystal. Mostoller and Rasolt [3], for example, introduced screened pair potentials for simple metal surfaces within the linear response theory. Morrison et al [4] investigated induced dipole contributions to the potential in the surface region of an ionic solid. However, the absence of reliable experimental data on such properties as surface, binding, adsorption and migration energies has greatly handicapped the development of such specifically designed surface potentials. The implementation of bulk based potentials had been the only reasonable alternative.

The pairwise interaction approach, where only two-body forces are

taken into account, appears to be widespread in surface science [5]. Mostly preference is given to potentials of a simple mathematical form, like the Lennard-Jones (6-12) pair potential [6,7,8,9].

During the last 20 to 30 years computer simulation techniques have also been used extensively to achieve understanding of surface phenomena. Bacigalupi and Neustadter [7] applied the Lennard-Jones (6-12) interaction potential to the calculation of adsorption energy of an atom at each of a network of sites within a surface unit cell for each of the eight highest surface density planes of an fcc crystal. Broughton and Gilmer [6] calculated surface excess free energies and stresses for the (111), (100) and (110) faces of an fcc crystal using molecular dynamics techniques. These authors also applied the latter technique to study three aspects of the crystal-fluid interface, viz. the bulk properties [10], structures of the fcc (111), (100) and (110) crystal-vapour interfaces [11], as well as the dynamical properties of fcc crystal-vapour systems [12]. L.C.A. Stoop [13] employed Monte Carlo techniques in an investigation of the lateral interactions within a silver monolayer on a W(110) surface. Snyman and Snyman [14] proposed a simple parameterised and truncated Fourier representation for the substrate interaction potential on the (111) face of an fcc metal. This was used in a model to attempt to relate, at atomic level, the orientation of the adatoms in an epitaxial overgrowth monolayer to the physical properties of the adatoms and that of the substrate. Bruch and Venables [15] developed a theoretical description of the distorted structures in adlayer lattices in terms of the amplitudes of the Fourier expansion of the adatom-substrate interaction potential. It was also shown

by W.A. Steele [8] that the interaction potential of a gas atom with a solid whose surface consists of a single type of exposed lattice plane, can be expressed as a two-dimensional Fourier series within a plane parallel to the surface.

Indeed, there are many problems whose solution would be greatly facilitated if an analytical representation for the adatom-substrate interaction potential were available, particularly if the potential were expressed as a Fourier series [8]. Such a problem is, for example, that of predicting the angular distribution of atoms in an atomic beam which is scattered from a crystal surface. A Fourier expansion of the potential is also necessary in the evaluation of the thermodynamic properties of adsorbed atoms. These properties are obtained from integrals (partition functions) of functions of the energy of atom-solid interaction, gas-solid interaction and the atom-atom interaction for clusters of atoms on the surface. The computation of bound-state energies of atoms on rare gas crystalline substrates, or exposed graphite basal planes, will be greatly facilitated by the existence of a Fourier series representation of the interaction potential.

Knowledge of the (numerical) value of the Fourier coefficients is also of the utmost importance in the theory of epitaxy [16]. In this phenomenon (epitaxy) the orientation of a single crystal B which grows on the surface of a single crystal A is primarily determined by the atomic arrangement of the surface of A on which growth proceeds. As growth is an adatom-by-adatom process the B atoms will be preferably adsorbed at the minima of the atom (B)-crystal (A) interaction potential. The theory shows that each

Fourier term competes for a specific orientation of crystal B and that the competing strength is the larger the larger the relevant Fourier coefficient [17]. Epitaxy is not only of fundamental but also of great technological interest as it is used in electronic and optoelectronic devices.

The present study is restricted to the problem of determining a Fourier series representation of the (gas) atom-crystal interaction potential energy on a single crystalline surface; specifically the interaction energy of an argon atom with the (001) face of an argon crystal. A Lennard-Jones type pairwise interaction model is used to simulate the interaction between the gas atom and the substrate. In this study the dependence of the interaction energy on both the distance from the surface and the displacement parallel to the surface are investigated. The dependence of the gas-solid potential on the perpendicular distance is accommodated implicitely in the Fourier approximation by allowing relaxation of an adatom only in a direction perpendicular to the crystal surface. Thus the computed two-dimensional Fourier series is an approximation of the *equilibrium* interaction potential.

A detailed description of the model, used in the present study, is given in Chapter 2. Chapter 3 contains a description of the numerical procedure adopted. The numerical results of computer experiments are presented and discussed in Chapter 4, with particular emphasis on the derived quantities, e.g. desorption and activation energy. An elaboration on the importance of the technique developed here and its wider application in surface science is also given.

2. THE MODEL

2.1. Introduction

In this chapter the origin and form of attractive, as well as repulsive forces between atoms of the rare gas elements are discussed. After considering the effect of many-body forces and quantum effects, the Lennard-Jones (6-12) pairwise potential is chosen as a realistic interaction potential to model the interaction between argon atoms. The merit of using a bulk based potential like the Lennard-Jones (6-12) potential in studying surface properties, is mentioned.

Furthermore a detailed exposition of the model is given with particular reference to representation of the surface and the equilibrium interaction potential of a reference atom above the surface of a crystalline substrate.

It is shown that, under the same symmetry conditions, the Fourier series representation of the equilibrium interaction potential derived using the physical approach of the reciprocal lattice is equivalent to the representation obtained by following a purely mathematical approach. A Fourier series representation of the same form as that of the equilibrium interaction potential is also derived for the equilibrium height.

2.2. Interatomic interaction: Lennard-Jones (6-12) pair potential

In many respects the inert gases with their closed-shell electron configurations form the simplest known crystals. The solid noble gases, except for helium, all crystallise in monatomic fcc Bravais lattices. The electron configuration of each atom is only slightly deformed in the solid.

The existence of condensed phases for the rare gas elements shows that there are attractive interactions between closed-shell atoms. These attractive forces, the so-called van der Waals or fluctuating dipole forces, are very weak. Qualitatively the physical origin of these cohesive forces arises from the fact that the charge distributions on the atoms in the crystal are not rigid. Although the average charge distribution in a single rare gas atom is spherically symmetric, at any instant there may be a net electric dipole moment as the electrons are in motion around the nucleus. The time-average electric moments nevertheless should vanish. The instantaneous dipole moment of magnitude p_1 of one atom induces an electric field $\underline{E}$ of magnitude $2p_1/r^3$ at the centre of a second atom at a distance r from the centre of the first atom. This electric field will in turn induce an instantaneous dipole moment of magnitude p_2, proportional to p_1 on the second atom, i.e.

$$p_2 = \alpha E = 2\alpha p_1/r^3 \ . \qquad (2.1)$$

The constant of proportionality α is known as the electronic polarizability, and is, by the above definition, the dipole moment per unit electric field. Since two dipoles have an energy of interaction proportional to the product of their moments divided by the cube of the distance between them [18], the potential energy of the dipole moments may be written as

$$U(r) \approx - \frac{1}{4\pi\varepsilon_0} \left[\frac{2p_1 p_2}{r^3}\right] = - \frac{1}{\pi\varepsilon_0} \left[\frac{\alpha p_1^2}{r^6}\right], \qquad (2.2)$$

where ε_0 is the permittivity of free space. The minus sign is characteristic of attractive interaction. Since the potential energy is proportional to p_1^2, its time-average does not vanish, although the

average value of p_1 is zero.

In general the interaction is expressed as [22]

$$U(r) = -\frac{C}{r^6} \quad . \tag{2.3}$$

Because of the r^{-6} dependence the interaction falls off rapidly with distance, and the force of interaction is very weak. This explains the low melting and boiling points of the condensed noble gases [19].

The interaction between two noble gas atoms also has a repulsive component, arising primarily from the overlap of electronic charge distributions as two atoms approach one another closely. The repulsive interaction can be understood in terms of the Pauli exclusion principle. According to this principle no two electrons can be in the same quantum state. Thus, the electron distributions of closed-shell atoms can overlap only if some of the electrons are partially promoted to unoccupied higher energy states, thereby increasing the total energy of the system. This introduces a repulsive contribution to the interaction [23].

Two forms of the repulsive part of the interatomic potential which most commonly appear in the literature are the Born-Mayer [25] potential and the repulsive term of the Lennard-Jones potential. The Born-Mayer potential has an exponential dependence and is given by

$$\phi_R(i,j) = Cb_ib_j \exp(-r_{ij}/0,345), \tag{2.4}$$

where $C \equiv 10^{-12}$ erg and b_i and b_j are characteristic constants

associated with the interacting atoms i and j respectively. The repulsive term of the Lennard-Jones (6-12) potential [26] is given by

$$\phi(r) = \frac{B}{r^{12}} , \tag{2.5}$$

where B is a positive constant and r is the distance between centres of mass of the two atoms. The exponential Born-Mayer potential has the undesirable property that it approaches a finite value as r approaches zero. This is quite unrealistic [27] since the nuclei of the two atoms cannot occupy the same space. The repulsive term (2.5) and the attractive term (2.3) constitute a simple but nevertheless realistic representation of the interaction potential of two spherical non-polar particles, like two inert gas atoms. The total potential energy of two atoms at separation r is usually written as

$$\phi(r) = 4\varepsilon \left[\left(\frac{\sigma}{r}\right)^{12} - \left(\frac{\sigma}{r}\right)^{6} \right] , \tag{2.6}$$

where ε is the depth of the potential well and σ is the distance at which $\phi(r) = 0$. The dependence of ϕ on r is illustrated in Fig. 2.1.

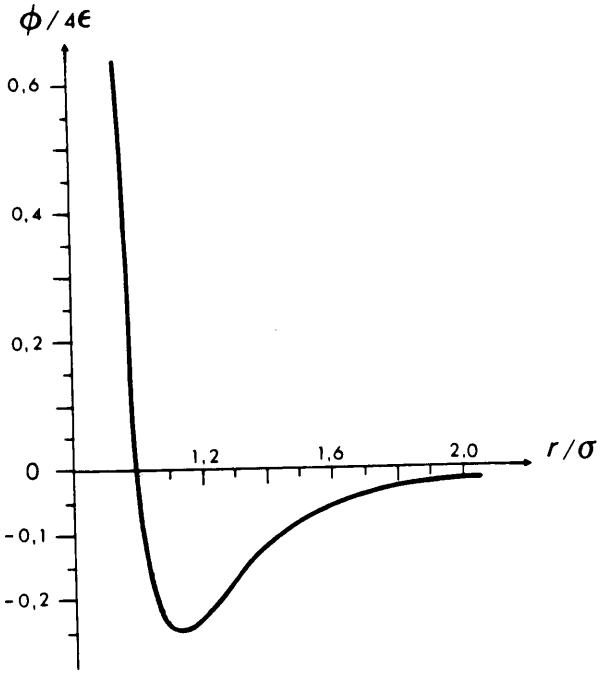

Fig. 2.1. The Lennard-Jones (6-12) potential (Eq. 2.6) [21].

It must be stressed that the exponent of the repulsive term was chosen to be 12 purely on the grounds that the number must be larger than 6 to allow for repulsion as r tends to zero and that with this choice the thermodynamic properties of neon, argon, krypton and xenon in the gas phase could be well reproduced by this potential using suitable values for the empirical parameters ε and σ [28]. These parameters can be determined experimentally from independent measurements in the gas phase. In addition, the analytic simplicity resulting from such a choice is definitely also a great advantage.

A Lennard-Jones (6-12) pairwise potential will be used in this study to model interaction between argon gas atoms. Although consideration of only two-body interactions seems to give a good description of the interaction potential in the case of rare gas atoms in the gas phase, caution must be exercised when considering its application to rare gas solids. At higher particle densities the interaction between the atoms in the crystal cannot accurately be represented as the sum of pair potentials. It is essential that many-body interactions be taken into account as well.

In the case of argon excellent agreement with the thermodynamic properties of the condensed phase is obtained if in addition third-order triple dipole (Axilrod-Teller-Muto) three-body interactions are included [29]. It has been shown that third-order dipole-quadrupole interactions and fourth-order triple-dipole interactions [30] make small contributions which fortuitously seem to cancel out almost completely [31] in calculations of the properties of liquid argon. It has also been suggested that the Lennard-Jones potential should be regarded as an *effective* pair potential rather than as a *true* pair

potential [32,33]. This is particularly true in the case of argon.

In spite of the call for caution it is generally agreed [34,35] that the pairwise interaction represented by the Lennard-Jones (6-12) potential dominates in the case of an argon atom on an argon crystal. It is therefore justified, also in view of mathematical simplicity, to ignore the second order contributions of many-body interactions in the model being used in this study.

The values of the parameters ε and σ which are used in the calculation of the interaction potential are those recommended by Mourits and Rummens [36]. In Table I values for the ε and σ, for argon, obtained from gas viscosities, as well as correlation techniques are listed.

TABLE I

Lennard-Jones parameters σ (in Å) for argon based on viscosity and calculated by empirical correlations, and recommended values for σ and ε (in eV) [36].

	ORIGIN	σ(in Å)	ε (in eV)
Viscosity based values	Franck	3,426	
	Hirschfelder et al	3,442	
	Svehla	3,542	
	Tee, Gotoh and Stewart	3,434	
	Linakis and Bowrey	3,320	
	Halkiadakis and Bowrey	3,302	
Calculated by emperical correlations	Stiel and Thodos	3,460	
	Tee, Gotoh and Stewart	3,432	
Recommended values	Mourits and Rummens	3,465	$9,7803 \times 10^{-3}$

The values that were used to determine the recommended values are italicised in Table I. These parameters were considered reliable and they form a basis with which the calculated parameters are compared.

Quantum kinetic energy also plays a role of varying importance in determining the total cohesive energy of the rare gas solids and consequently in determining the potential above the solid. Even at zero temperature the ion cores of the noble gas atoms cannot be perfectly localised with zero kinetic energy at the lattice points, as this violates the Heisenberg uncertainty principle. If an ion core is confined to a region Δx in one dimension, then, according to the uncertainty principle, the related spread in momentum $\Delta(mv)$ will be at least equal to $h/2\pi\Delta x$, where h is Planck's constant the kinetic energy of the core will then be of order $h^2/M(\Delta x)^2$, where M is the mass of the core. This energy is known as zero-point kinetic energy. It makes a positive contribution towards the cohesive energy and reduces the binding. However, zero-point kinetic energy becomes less important with increasing mass as is illustrated by the value of 0,19 for the de Boer parameter [20] Λ for Argon. The de Boer parameter is a measure of the importance of quantum effects in noble gases. The de Boer parameter squared, Λ^2, is roughly the ratio of the *kinetic energy* of zero-point motion of an atom to the value of the attractive interaction energy. It is clear that the value of the zero-point kinetic energy is only about 3,61% of that due to the attractive component of the Lennard-Jones (6-12) potential. Thus, the effect of zero-point motion is comparatively small in the case of argon and neglecting this effect still yields a realistic model.

The usefulness of simple potentials like the Lennard-Jones (6-12) potential in studying various bulk properties has been established beyond doubt. However, extending their application to surface problems is questionable as atoms in the surface layer do not experience the same forces as those in the bulk. This imbalance of forces induces displacements and polarizations of the atoms near the surface of a crystal. If more precise calculations are to be performed, a specifically designed surface potential should be used. Experimental data on properties like surface, binding and adsorption energies on which such a potential could be based, is neither readily available, nor reliable. From the literature it appears that no suitable simple surface potential exists. Consequently, the Lennard-Jones (6-12) bulk pair potential, of which the shortcomings have already been acknowledged, will be employed here to approximate the interatomic interactions both in the crystal and on the surface.

2.3. Surface representation

In the present study possibly the simplest representation of a surface is assumed, namely that of a "rigid planar array of exposed atoms having the same stoichiometry, lattice spacing and lattice symmetry as the bulk" [37]. No attempt will be made to take into account the surface phenomena of multilayer relaxation or surface reconstruction. This should not affect the realism of the model too severely as low-energy diffraction data for clean fcc metal surfaces [38,39] indicates that there is little relaxation on the {100} surface. Relaxation calculations made by R.A. Johnson [39], using a model based on nearest-neighbour central forces and volume-dependent energy terms, suggested that the

displacement of the {100} surface plane in an fcc metal is zero. As argon also crystallises in an fcc Bravais lattice, it is reasonable to assume that there will be very little relaxation on the {001} surface of such a crystal.

In the present model the x-y Cartesian reference plane passes through the centres of the {001} surface atoms. The origin O is fixed at a point lying at the centre of a surface atom. The x-axis extends along a row of atoms spaced a distance $\ell = a/\sqrt{2}$ apart, a being the lattice constant. The z-axis is positive along the outward normal. (See Fig. 2.2.). The position of an atom A in the crystal, as depicted in Fig. 2.2, is given by

$$A(x_A, y_A, z_A) = \begin{cases} (\ell I,\ \ell J,\ aK/2); & K \text{ even or zero} \\ (\ell I,\ \ell J,\ aK/2) + (\ell/2,\ \ell/2,\ 0); & K \text{ uneven.} \end{cases} \tag{2.7}$$

The crystal to be referred to as the substrate is modelled by a rigid lattice of point particles interacting independently with a reference adatom at P according to a 6-12 Lennard-Jones pairwise potential. The energy contributions are accordingly additive. If ϕ_{PJ} is the value of ϕ for the interaction between the adatom at $P(x_P, y_P, z_P)$ and an atom at $J(x_J, y_J, z_J)$ in the substrate at a distance R_{PJ} from P, ϕ_{PJ} may be computed using (2.6) and (2.7):

$$\phi_{PJ} = 4\epsilon \left[\left(\frac{\sigma}{R_{PJ}}\right)^{12} - \left(\frac{\sigma}{R_{PJ}}\right)^{6}\right], \tag{2.8}$$

where

$$R_{PJ} = \sqrt{(x_P - x_J)^2 + (y_P - y_J)^2 + (z_P - z_J)^2}\ . \tag{2.9}$$

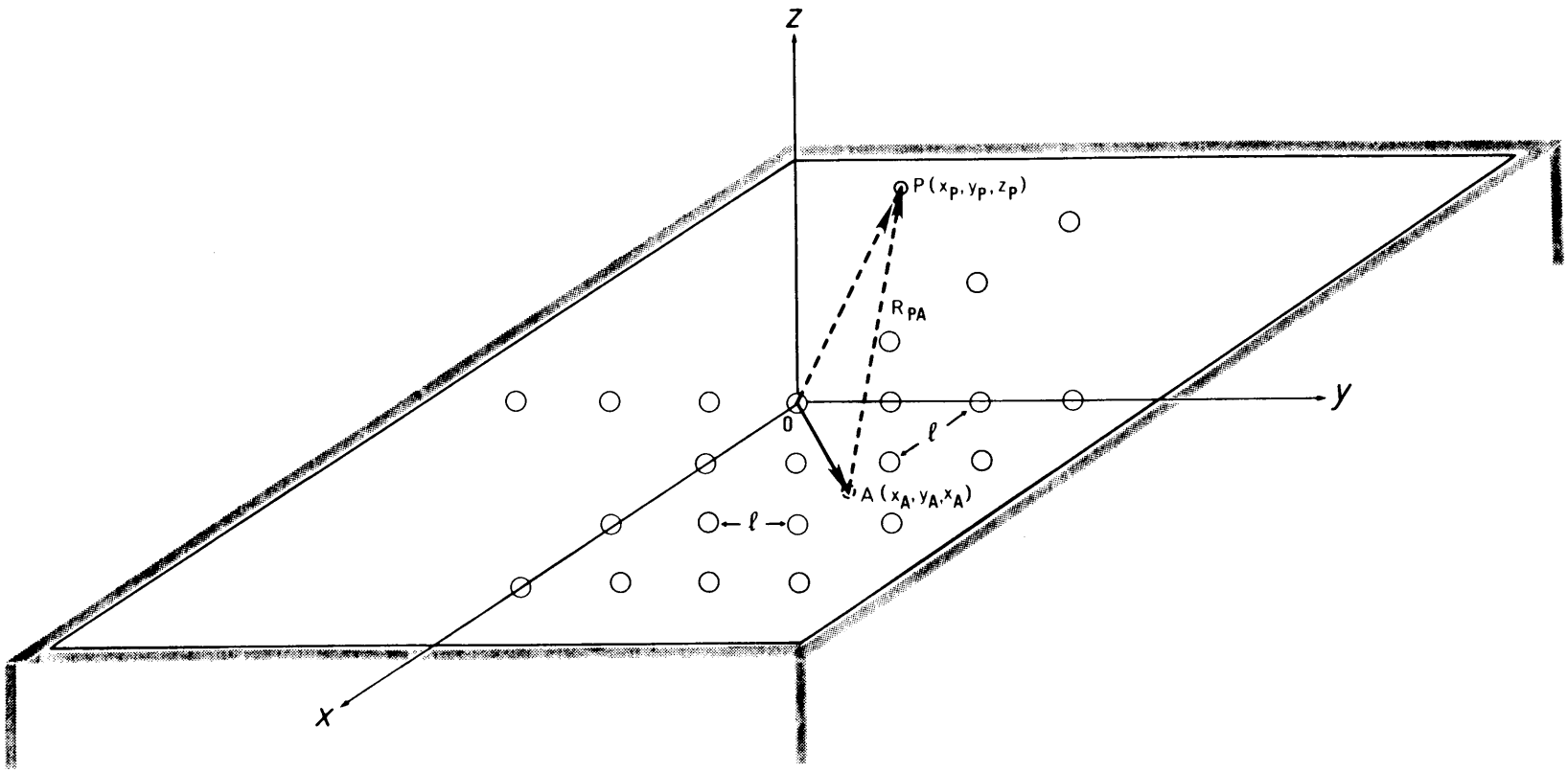

Fig. 2.2. Diagram indicating the relative positions of the reference adatom P above the crystal substrate and an arbitrary atom A in the crystal substrate with respect to the chosen system of axes.

The total energy of the reference atom at P is thus given by

$$\phi_P = \sum_J \phi_{PJ} \, , \qquad (2.10)$$

where the summation is taken over all the atoms in the substrate. In the actual computation a cutt-off radius R = 5a, where a is the lattice parameter for argon, was introduced setting ϕ_{PJ} equal to zero for $R_{PJ} > R$. This approximation is needed because of computational limitations and is justified by the fact that an increase of the cut-off radius from 5a to 6a increases the calculated equilibrium interaction energy of an atom at the origin by less than 0,3%. The adoption of a comparatively small cut-off radius reduces the computational time considerably. Thus the part of the solid argon crystal substrate which effectively generates the potential at a point near the origin, is in the form of a hemisphere with radius 5a as depicted in Fig. 2.3(a).

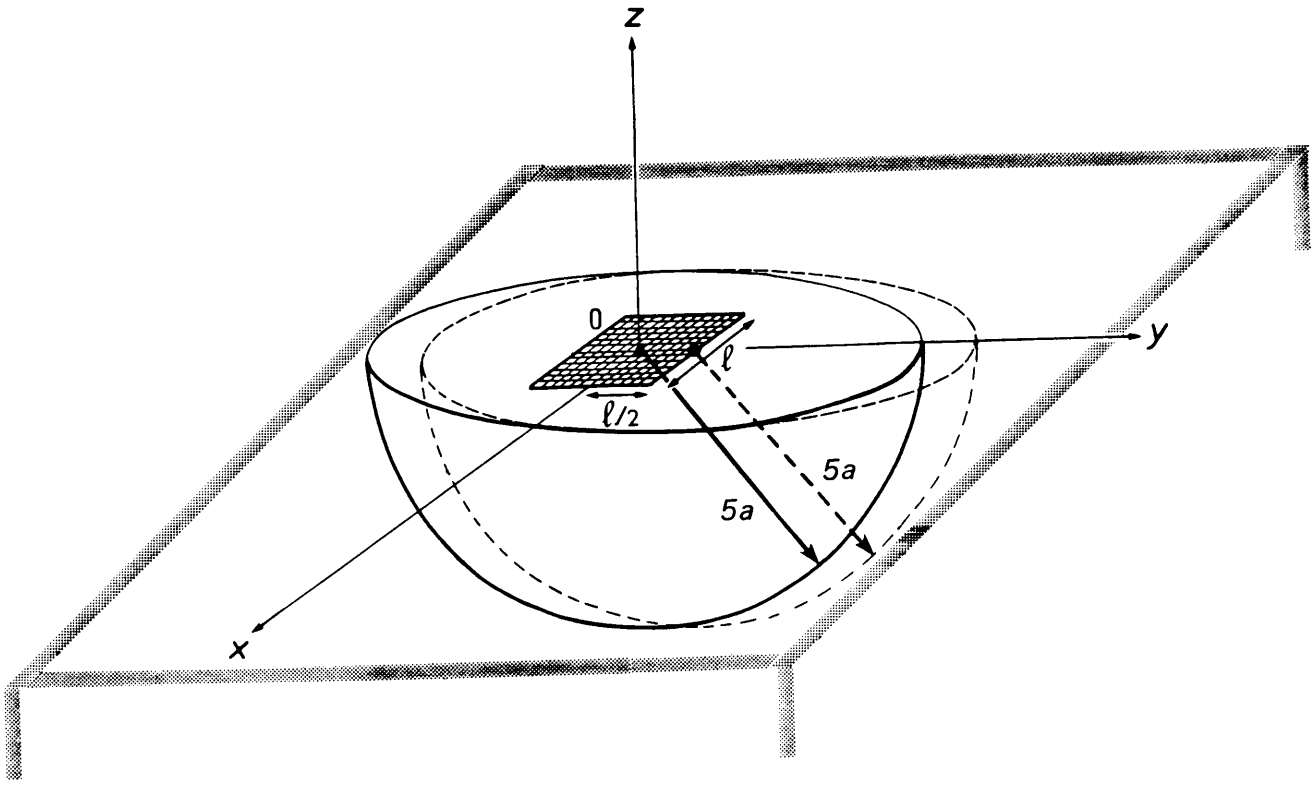

Fig. 2.3(a) The cut-off distance is taken 5a for all positions considered in the unit cell.

2.4. Equilibrium interaction potential

The equilibrium interaction potential near the surface of the crystal may now in principle be computed in the following manner: The two-dimensional surface unit cell, with side length ℓ, is overlayed by a mesh of grid points as shown in figure 2.3(a) and (b). At each of these grid points (x,y) and at a fixed height z above the surface, the interaction potential $\phi_{xy}(z)$ of a reference atom with the atoms of the substrate in the hemispherical region below may be calculated using equations (2.8) and (2.10). Clearly $\phi_{xy}(z)$ will vary with z (see Fig. 2.4) and the equilibrium interaction potential, i.e. $\phi_{xy}(z_{min})$ = minimum, occurs at a height z_{min} defined by

$$\left(\frac{d\phi_{xy}}{dz}\right)_{z_{min}} = 0. \qquad (2.11)$$

In practice the value of z_{min} and therefore also of the equilibrium interaction potential $\phi_{xy}(z_{min})$ is determined by allowing the reference atom to vary its position in the z-direction until the minimum value of $\phi_{xy}(z)$ is attained. (See Fig. 2.3(b)).

Thus for each grid point (x_i,y_j), i = 1, ..., n and j = 1, ..., m a $z_{min}(x_i,y_j)$ and an associated $\phi_{x_iy_i}(z_{min})$ are computed. We now define the set of values

$$\phi_e(x_i,y_j) = \phi_{x_iy_i}(z_{min}). \qquad (2.12)$$

The discrete values $\phi_e(x_i,y_j)$ may now be used as data for the calculation of the Fourier coefficients of a two-dimensional Fourier series

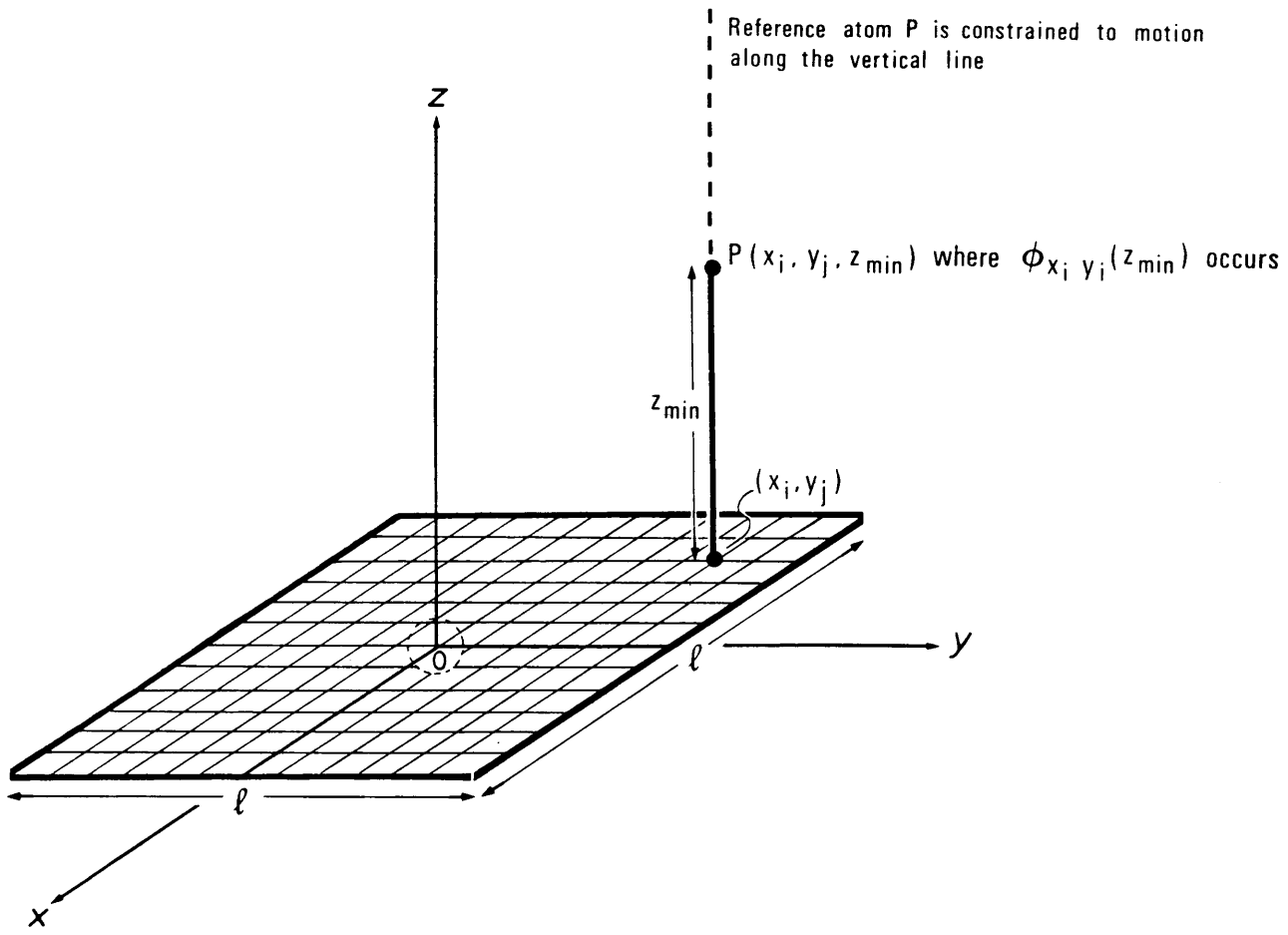

Fig. 2.3(b) The two-dimensional surface unit cell is overlayed by a mesh of grid points and the reference atom P is constrained to motion along vertical lines passing through the grid points.

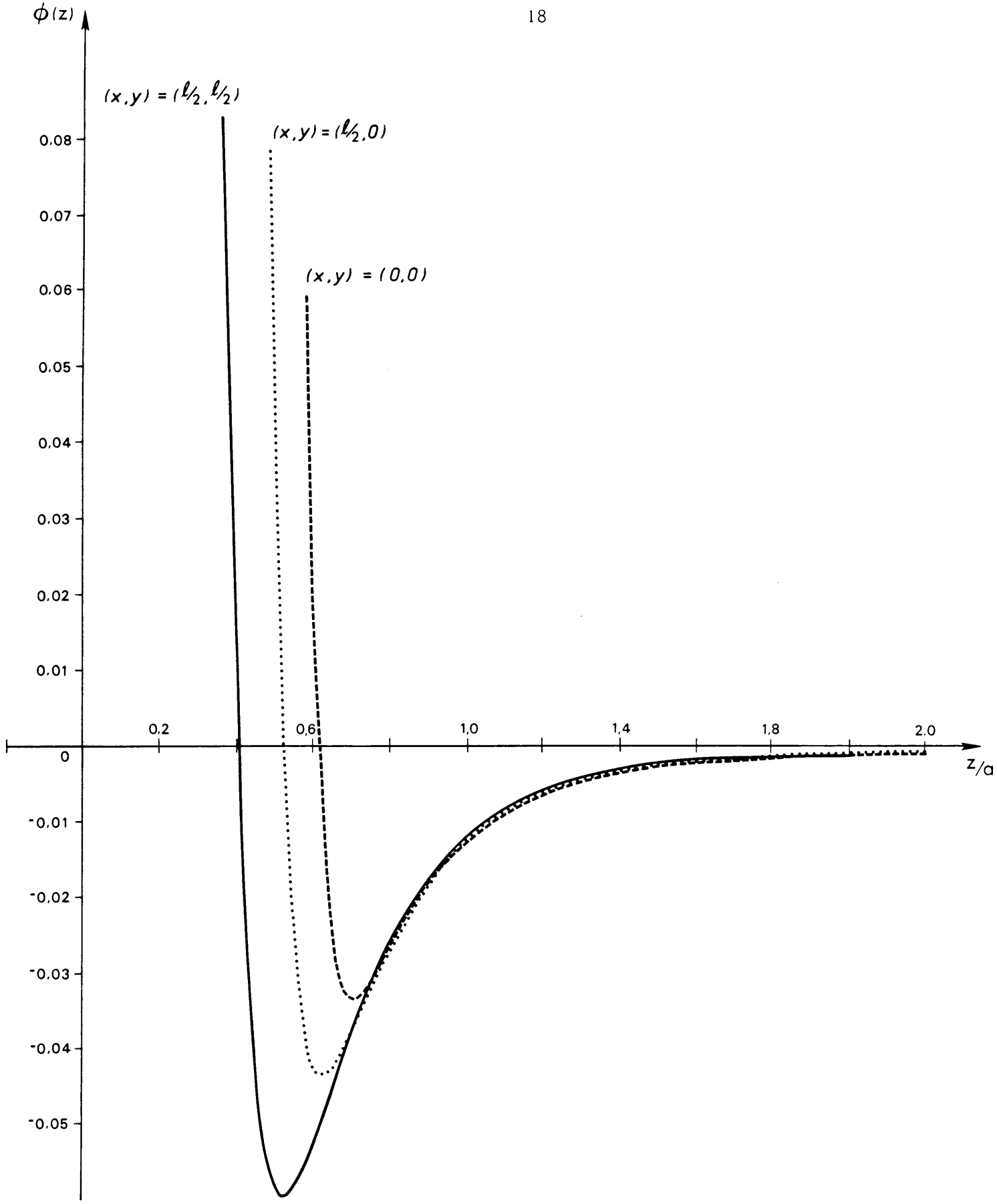

Fig. 2.4. Variation of potential energy of an atom along the vertical for three positions in the surface unit cell of the {001} face of an fcc lattice.

representation of $\phi_e(x,y)$, the equilibrium interaction potential, varying continuously with position (x,y).

Similarly, a continuous Fourier series representation of the surface $z_{min}(x,y)$, of minimum potential energy, can also be calculated from the discrete values $z_{min}(x_i,y_j)$.

Details of the way in which the Fourier coefficients are calculated are given in Chapter 3.

2.5. Fourier series representation of the equilibrium interaction potential $\phi_e(x,y)$

In deciding on a form for a two-dimensional Fourier series representation of the equilibrium interaction potential $\phi_e(x,y)$, the inherent symmetry of the argon crystal surface must be taken into account. The symmetry of the model is reflected by relationships that exist for the Fourier coefficients. From a practical point of view, it is desirable to retain only the linearly independent coefficients in a Fourier series representation of $\phi_e(x,y)$ as this will greatly reduce the computational effort. The derivation of such a Fourier series representation can be approached in two ways, either from a physical or from a purely mathematical point of view. Both these approaches will be considered.

2.5.1. The symmetry of the model

In the present model it is assumed that the argon crystal is a semi-infinite perfect crystal, the atomic arrangement forming a regular

array. The {001} substrate surface of the fcc crystal may accordingly be represented by a square two-dimensional unit cell, repeating itself with period $\ell = a/\sqrt{2}$ along the $<110>$ and $<\bar{1}10>$ directions as shown in Fig. 2.5. These directions are respectively chosen as the x and y directions for the two-dimensional Fourier series representation of the surface potential. It is reasonable to assume that the equilibrium interaction potential should be a periodic function with the same periodicity and symmetry as the Bravais lattice of the underlying substrate surface. This lattice has a fourfold rotational symmetry. Thus the following conditions hold for the equilibrium interaction potential $\phi_e(x,y)$:

$$\phi_e(x,y) = \phi_e(-x, -y), \tag{2.13a}$$

$$\phi_e(x,y) = \phi_e(-y, x) , \tag{2.13b}$$

and

$$\phi_e(x,y) = \phi_e(y, -x). \tag{2.13c}$$

Equation (2.13c) is implied by (2.13a) and (2.13b). From equation (2.13a) it is clear that $\phi_e(x,y)$ is an even function. A further symmetry condition exists in the argon crystal lattice, viz. a mirror plane passing through the origin. (See Fig. 2.5). With a twofold axis and one mirror plane, there is automatically a second mirror plane normal to the first. The implications for $\phi_e(x,y)$ are that

$$\phi_e(x,y) = \phi_e(x, -y) \tag{2.14a}$$

and

$$\phi_e(x,y) = \phi_e(-x, y). \tag{2.14b}$$

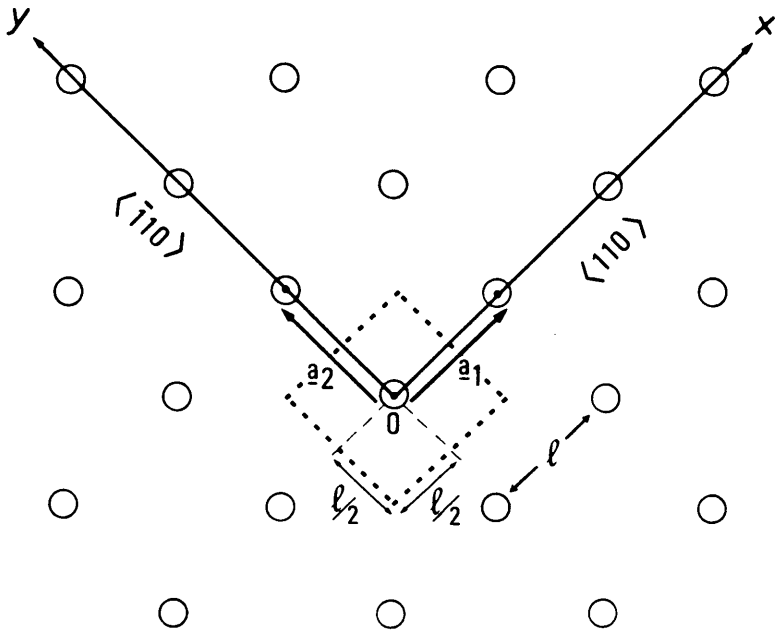

Fig. 2.5. The {001} surface of an fcc crystal. $\underline{a}_1$ and $\underline{a}_2$ are chosen as primitive surface vectors in real physical space.

2.5.2. The mathematical approach

According to Weinberger [40] any continuously differentiable function f(x,y) of two variables periodic with period 2π in both variables i.e.

$$f(x + 2\pi, y) = f(x, y + 2\pi) = f(x,y) \tag{2.15}$$

has a uniformly convergent Fourier series

$$\begin{aligned} f(x,y) = \frac{1}{4} a_{oo} &+ \frac{1}{2} \sum_{m=1}^{\infty} [a_{om} \cos my + b_{om} \sin my] \\ &+ \frac{1}{2} \sum_{n=1}^{\infty} [a_{no} \cos nx + c_{no} \sin nx] \\ &+ \sum_{n=1}^{\infty} \sum_{m=1}^{\infty} [a_{nm} \cos nx \cos my + b_{nm} \cos nx \sin my \\ &+ c_{nm} \sin nx \cos my + d_{nm} \sin nx \sin my] \end{aligned} \tag{2.16}$$

with

$$a_{nm} = \frac{1}{\pi^2}\int_{-\pi}^{\pi}\int_{-\pi}^{\pi} f(x, y)\cos nx \cos my dxdy,$$

$$b_{nm} = \frac{1}{\pi^2}\int_{-\pi}^{\pi}\int_{-\pi}^{\pi} f(x, y)\cos nx \sin my dxdy,$$

$$c_{nm} = \frac{1}{\pi^2}\int_{-\pi}^{\pi}\int_{-\pi}^{\pi} f(x, y)\sin nx \cos my dxdy, \qquad (2.17)$$

$$d_{nm} = \frac{1}{\pi^2}\int_{-\pi}^{\pi}\int_{-\pi}^{\pi} f(x, y)\sin nx \sin my dxdy.$$

For a function F(x,y) which is periodic with period 1 in both x and y (normalized coordinates) the Fourier series will be of the form

$$\begin{aligned} F(x,y) = \frac{1}{4}a_{oo} &+ \frac{1}{2}\sum_{m=1}^{\infty}[a_{om}\cos 2\pi my + b_{om}\sin 2\pi my] \\ &+ \frac{1}{2}\sum_{n=1}^{\infty}[a_{no}\cos 2\pi nx + c_{no}\sin 2\pi nx] \\ &+ \sum_{n=1}^{\infty}\sum_{m=1}^{\infty}[a_{nm}\cos 2\pi nx\cos 2\pi my + b_{nm}\cos 2\pi nx\sin 2\pi my \\ &\quad + c_{nm}\sin 2\pi nx\cos 2\pi my + d_{nm}\sin 2\pi nx\sin 2\pi my], \end{aligned} \qquad (2.18)$$

where the relationship between the normalised and absolute coordinates (x',y') are given by $x = x'/\ell$ and $y = y'/\ell$. The constants in equation (2.18) are of the forms:

$$a_{nm} = 4\int_{-\frac{1}{2}}^{\frac{1}{2}}\int_{-\frac{1}{2}}^{\frac{1}{2}} F(x,y)\cos 2\pi nx\cos 2\pi my dxdy,$$

$$b_{nm} = 4\int_{-\frac{1}{2}}^{\frac{1}{2}}\int_{-\frac{1}{2}}^{\frac{1}{2}} F(x,y)\cos 2\pi nx\sin 2\pi my dxdy,$$

$$c_{nm} = 4\int_{-\frac{1}{2}}^{\frac{1}{2}}\int_{-\frac{1}{2}}^{\frac{1}{2}} F(x,y)\sin 2\pi nx\cos 2\pi my dxdy, \qquad (2.19)$$

$$d_{nm} = 4\int_{-\frac{1}{2}}^{\frac{1}{2}}\int_{-\frac{1}{2}}^{\frac{1}{2}} F(x,y)\sin 2\pi nx\sin 2\pi my dxdy.$$

If in addition $F(x,y)$ is an even function, it follows from the above that the constants $b_{nm} = 0 = c_{nm}$, and that the constants $b_{om} = 0 = c_{no}$.

Thus

$$F(x,y) = \frac{1}{4} a_{oo} + \frac{1}{2} \sum_{m=1}^{\infty} a_{om} \cos 2\pi my + \frac{1}{2} \sum_{n=1}^{\infty} a_{no} \cos 2\pi nx + \sum_{n=1}^{\infty} \sum_{m=1}^{\infty} [a_{nm} \cos 2\pi nx \cos 2\pi my + d_{nm} \sin 2\pi nx \sin 2\pi my] . \tag{2.20}$$

Suppose $F(x,y) = F(-y,x)$. Then

$$\frac{1}{4} a_{oo} + \frac{1}{2} \sum_{m=1}^{\infty} a_{om} \cos 2\pi my + \frac{1}{2} \sum_{n=1}^{\infty} a_{no} \cos 2\pi nx + \sum_{n=1}^{\infty} \sum_{m=1}^{\infty} [a_{nm} \cos 2\pi nx \cos 2\pi my + d_{nm} \sin 2\pi nx \sin 2\pi my]$$

$$= \frac{1}{4} a_{oo} + \frac{1}{2} \sum_{m=1}^{\infty} a_{om} \cos 2\pi mx + \frac{1}{2} \sum_{n=1}^{\infty} a_{no} \cos 2\pi n(-y) + \sum_{n=1}^{\infty} \sum_{m=1}^{\infty} [a_{nm} \cos 2\pi n(-y) \cos 2\pi mx + d_{nm} \sin 2\pi n(-y) \sin 2\pi mx] . \tag{2.21}$$

The above implies that the Fourier coefficients satisfy certain symmetry relationships. By comparing the first two series on both sides of equation (2.21) it follows that

$$a_{oi} = a_{io} \equiv c_i, \qquad i = 1,2, \ldots \infty . \tag{2.22}$$

Now consider the last series on the right hand side of equation (2.21) and change dummy indices:

$$\sum_{n=1}^{\infty}\sum_{m=1}^{\infty}\left[a_{nm}\cos 2\pi n(-y)\cos 2\pi mx + d_{nm}\sin 2\pi n(-y)\sin 2\pi mx\right]$$

$$= \sum_{n=1}^{\infty}\sum_{m=1}^{\infty}\left[a_{nm}\cos 2\pi ny\cos 2\pi mx + d_{nm}\sin 2\pi n(-y)\sin 2\pi mx\right]$$

$$= \sum_{m=1}^{\infty}\sum_{n=1}^{\infty}\left[a_{mn}\cos 2\pi my\cos 2\pi nx + d_{mn}\sin 2\pi m(-y)\sin 2\pi nx\right]$$

$$= \sum_{m=1}^{\infty}\sum_{n=1}^{\infty}\left[a_{mn}\cos 2\pi my\cos 2\pi nx - d_{mn}\sin 2\pi my\sin 2\pi nx\right]. \qquad (2.23)$$

By comparing the last series on the left hand side of equation (2.21) with equation (2.23), it is seen that

$$a_{nm} = a_{mn}$$

and (2.24)

$$d_{nm} = -d_{mn}.$$

On using the relation (2.22), equation (2.20) reduces to

$$F(x,y) = \frac{1}{4}a_{oo} + \frac{1}{2}\sum_{m=1}^{\infty}c_m\cos 2\pi my + \frac{1}{2}\sum_{n=1}^{\infty}c_n\cos 2\pi nx + \sum_{n=1}^{\infty}\sum_{m=1}^{\infty}\left[a_{nm}\cos 2\pi nx\cos 2\pi my + d_{nm}\sin 2\pi nx\sin 2\pi my\right] \qquad (2.25)$$

If furthermore

$$F(x,y) = F(x,-y) \qquad (2.26a)$$

and

$$F(x,y) = F(-x,y), \qquad (2.26b)$$

and condition (2.26b) is applied to equation (2.25), we obtain:

$$F(x,y) = \frac{1}{4} a_{oo} + \frac{1}{2} \sum_{m=1}^{\infty} c_m [\cos 2\pi my + \cos 2\pi mx]$$

$$+ \sum_{n=1}^{\infty} \sum_{m=1}^{\infty} [a_{nm} \cos 2\pi nx \cos 2\pi my + d_{nm} \sin 2\pi nx \sin 2\pi my]$$

$$= \frac{1}{4} a_{oo} + \frac{1}{2} \sum_{m=1}^{\infty} c_m [\cos 2\pi my + \cos 2\pi m(-x)]$$

$$+ \sum_{n=1}^{\infty} \sum_{m=1}^{\infty} [a_{nm} \cos 2\pi n(-x) \cos 2\pi my + d_{nm} \sin 2\pi n(-x) \sin 2\pi my]$$

$$= F(-x,y) \qquad (2.27)$$

This reduces to

$$\sum_{n=1}^{\infty} \sum_{m=1}^{\infty} d_{nm} \sin 2\pi nx \sin 2\pi my = \sum_{n=1}^{\infty} \sum_{m=1}^{\infty} - d_{nm} \sin 2\pi n(x) \sin 2\pi my. \qquad (2.28)$$

By comparing the lefthand and righthand sides of the above equation it follows that

$$d_{nm} = - d_{nm}. \qquad (2.29)$$

This can only be true if $d_{nm} = 0$. The same result can be deduced by using equation (2.26a).

Thus a Fourier series representation for a function that has the same continuity and symmetry properties as the equilibrium interaction potential $\phi_e(x,y)$ must be of the form

$$F(x,y) = \frac{1}{4} a_{oo} + \frac{1}{2} \sum_{m=1}^{\infty} c_m (\cos 2\pi my + \cos 2\pi mx)$$

$$+ \sum_{n=1}^{\infty} \sum_{m=1}^{\infty} a_{nm} \cos 2\pi nx \cos 2\pi my. \qquad (2.30)$$

2.5.3. The physical approach

An identical representation for the potential may be obtained by adopting alternative arguments more in keeping with the philosophy of solid state physics and crystallography. In this approach, which is briefly dealt with below, the potential representation is developed via the reciprocal lattice of the crystal.

As a regular infinite perfect crystal substrate is assumed in the model, the equilibrium interaction potential $\phi_e(\underline{r})$ of an atom above the substrate, should be a periodic function with the periodicity of the Bravais lattice of the underlying substrate surface, i.e.

$$\phi_e(\underline{r} + \underline{T}) = \phi_e(\underline{r}), \qquad (2.31)$$

for all surface lattice vectors $\underline{T}$. Any function which is invariant under all surface lattice translations $\underline{T}$ may be expressed as a Fourie-series

$$n(\underline{r}) = \sum_{\underline{G}} n_{\underline{G}} e^{i\underline{G}\cdot\underline{r}}, \qquad (2.32)$$

where $\underline{G}$ is any reciprocal lattice translation vector in the two-dimensional reciprocal lattice and $\underline{r}$ is any surface vector in real space [24]. In particular

$$\phi_e(\underline{r}) = \sum_{\underline{G}} \phi_{e\underline{G}}\, e^{i\underline{G}\cdot\underline{r}} . \tag{2.33}$$

Consider Fig. 2.5. The vectors $\underline{a}_1 = \ell\hat{x}$ and $\underline{a}_2 = \ell\hat{y}$, where $\ell = \frac{a}{\sqrt{2}}$ and a is the lattice parameter, may be chosen as primitive surface vectors in real physical space. The reciprocal lattice vectors corresponding to $\underline{a}_1$ and $\underline{a}_2$ are given by

$$\underline{b}_1 = \frac{2\pi}{\ell}\,\hat{x} \qquad \text{and} \qquad \underline{b}_2 = \frac{2\pi}{\ell}\,\hat{y} . \tag{2.34}$$

Let $\underline{G} = h\underline{b}_1 + k\underline{b}_2$ and $\underline{r} = x\underline{a}_1 + y\underline{a}_2$, where the h,k are integers. It follows that

$$\underline{G}\cdot\underline{r} = 2\pi(hx + ky). \tag{2.35}$$

Hence

$$\phi_e(\underline{r}) = \sum_{\underline{G}} \phi_{e\underline{G}}\, e^{i\underline{G}\cdot\underline{r}} = \sum_{h,k} A_{hk} e^{2\pi i(hx+ky)} . \tag{2.36}$$

However, equation (2.36) can also be written as follows:

$$\begin{aligned}\sum_{h,k=-\infty}^{\infty} A_{hk} e^{i2\pi(hx+ky)} = \sum_{h,k=1}^{\infty} [\, & A_{hk} e^{i2\pi(hx+ky)} + A_{-h,-k} e^{-i2\pi(hx+ky)} \\ & + A_{-kh}\, e^{i2\pi(-kx+hy)} + A_{k,-h} e^{i2\pi(kx-hy)}] \\ & + \sum_{k=1}^{\infty} [A_{ok}\, e^{i2\pi ky} + A_{o,-k}\, e^{-i2\pi ky}] \\ & + \sum_{h=1}^{\infty} [A_{ho}\, e^{i2\pi hx} + A_{-ho}\, e^{-i2\pi hx}] + A_{oo}\end{aligned} \tag{2.37}$$

Applying the inversion symmetry condition (2.13a) to equation (2.36)

yields the result:

$$\sum_{h,k}^{\infty} A_{hk}\, e^{i2\pi(hx+ky)} = \sum_{h,k}^{\infty} A_{hk}\, e^{i2\pi[h(-x)+k(-y)]}$$

$$= \sum_{h,k}^{\infty} A_{hk}\, e^{-i2\pi(hx+ky)}$$

$$= \sum_{-h,-k}^{\infty} A_{-h,-k}\, e^{i2\pi(hx+ky)}\,, \tag{2.38}$$

from which it follows that

$$A_{hk} = A_{-h,-k}\,. \tag{2.39}$$

If now only those terms in the sum of which A_{hk} and $A_{-h,-k}$ are the coefficients are considered, we may write

$$A_{hk}\, e^{i2\pi(hx+ky)} + A_{-h,-k}\, e^{-i2\pi(hx+ky)}$$

$$= A_{hk}[\cos 2\pi(hx+ky) + i\sin 2\pi(hx+ky)] + A_{-h,-k}[\cos 2\pi(-h(x)+(-k)y)$$

$$+ i\sin 2\pi((-h)x+(-k)y)]$$

$$= A_{hk}[\cos 2\pi(hx+ky) + i\sin 2\pi(hx+ky)] + A_{-h,-k}[\cos 2\pi(hx+ky)$$

$$- i\sin 2\pi(hx+ky]$$

$$= A_{hk}[\cos 2\pi(hx+ky)] + A_{-h,-k}[\cos 2\pi(hx+ky)]$$

$$= 2A_{hk}\cos 2\pi(hx+ky)\,. \tag{2.40}$$

Similarly it follows that

$$A_{-kh}\, e^{i2\pi(-kx+hy)} + A_{k,-h}\, e^{i2\pi(kx-hy)} = 2A_{-kh} \cos 2\pi(-kx+hy) . \qquad (2.41)$$

In view of equations (2.40) and (2.41), the expression for the equilibrium interaction $\phi_e(x,y)$ simply becomes

$$\phi_e(x,y) = \sum_{h,k=1}^{\infty} 2A_{hk} \cos 2\pi(hx+ky) + \sum_{h,k=1}^{\infty} 2A_{-kh} \cos 2\pi(-kx+hy)$$

$$+ \sum_{k=1}^{\infty} [A_{ok}\, e^{i2\pi ky} + A_{o,-k}\, e^{-i2\pi ky}] + \sum_{h=1}^{\infty} [A_{ho}\, e^{i2\pi hx} + A_{-ho}\, e^{-i2\pi hx}]$$

$$+ A_{oo} \qquad (2.42)$$

Using the symmetry condition (2.13b), viz. $\phi_e(x,y) = \phi_e(-y,x)$, yields

$$\sum_{h,k=-\infty}^{\infty} A_{hk}\, e^{i2\pi(hx+ky)} = \sum_{h,k=-\infty}^{\infty} A_{hk}\, e^{i2\pi(-hy+kx)}$$

$$= \sum_{-h,k=-\infty}^{\infty} A_{-hk}\, e^{i2\pi(hy+kx)}$$

$$= \sum_{-k,h=-\infty}^{+\infty} A_{-kh}\, e^{i2\pi(ky+hx)} \qquad (2.43)$$

and it can be deduced that

$$A_{hk} = A_{-kh} . \qquad (2.44)$$

Thus equation (2.42) can be simplified further:

$$\phi_e(x,y) = \sum_{h,k=1}^{\infty} 2A_{hk}[\cos 2\pi(hx+ky) + \cos 2\pi(-kx+hy)]$$

$$+ \sum_{k=1}^{\infty} [A_{ok}\, e^{i2\pi ky} + A_{o,-k}\, e^{-i2\pi ky}] + \sum_{h=1}^{\infty} [A_{ho}\, e^{i2\pi hx} + A_{-ho}\, e^{-i2\pi hx}]$$

$$+ A_{oo}$$

$$\phi_e(x,y) = A_{oo} + \sum_{k=1}^{\infty} 2A_{ok} \cos 2\pi ky + \sum_{h=1}^{\infty} 2A_{ho} \cos 2\pi hx$$

$$+ \sum_{h,k=1}^{\infty} 2A_{hk}[\cos 2\pi(hx + ky) + \cos 2\pi(-kx + hy)]$$

$$= A_{oo} + \sum_{k=1}^{\infty} 2A_{ok} \cos 2\pi ky + \sum_{h=1}^{\infty} 2A_{ho} \cos 2\pi hx$$

$$+ \sum_{h,k=1}^{\infty} 2A_{hk}[\cos 2\pi hx \cos 2\pi ky - \sin 2\pi hx \sin 2\pi ky$$

$$+ \cos 2\pi kx \cos 2\pi hy + \sin 2\pi kx \sin 2\pi hy] . \qquad (2.45)$$

The first two series in equation (2.45) may be rewritten as follows:

$$\sum_{k=1}^{\infty} 2A_{ok} \cos 2\pi ky + \sum_{h=1}^{\infty} 2A_{ho} \cos 2\pi hx$$

$$= \frac{1}{2} \sum_{h=1}^{\infty} C_h(\cos 2\pi hy + \cos 2\pi hx) \qquad (2.46)$$

where

$$C_h = 4A_{oh} = 4A_{ho} .$$

Also for the last series in equation (2.45) we obtain:

$$\sum_{h,k=1}^{\infty} 2A_{hk}[\cos 2\pi hx \cos 2\pi ky - \sin 2\pi hx \sin 2\pi ky + \cos 2\pi kx \cos 2\pi hy + \sin 2\pi kx \sin 2\pi hy]$$

$$= \sum_{h,k=1}^{\infty} D_{hk} \cos 2\pi hx \cos 2\pi ky + \sum_{h,k=1}^{\infty} E_{hk} \sin 2\pi hx \sin 2\pi ky , \qquad (2.47)$$

where

$$D_{hk} = 2[A_{hk} + A_{kh}] \text{ and } E_{hk} = 2[-A_{hk} + A_{kh}] . \qquad (2.48)$$

It therefore follows that

$$\phi_e(x,y) = \frac{1}{4} D_{oo} + \frac{1}{2} \sum_{h=1}^{\infty} C_h[\cos 2\pi hx + \cos 2\pi hy] + \sum_{h,k=1}^{\infty} D_{hk} \cos 2\pi hx \cos 2\pi ky + E_{hk} \sin 2\pi hx \sin 2\pi ky] . \qquad (2.49)$$

If the two perpendicular mirror planes passing through the origin in the argon crystal lattice are taken into account, it follows that

$$E_{hk} = - E_{hk} \qquad (2.50)$$

and thus $E_{hk} = 0$. The simplest expression for the equilibrium interaction potential satisfying the symmetry conditions described in paragraph 2.5.1. is therefore:

$$\phi_e(x,y) = \frac{1}{4} D_{oo} + \frac{1}{2} \sum_{h=1}^{\infty} C_h(\cos 2\pi hx + \cos 2\pi hy)$$

$$+ \sum_{h,k=1}^{\infty} [D_{hk} \cos 2\pi hx \cos 2\pi ky] . \qquad (2.51)$$

By comparing equation (2.30) and (2.51) it is clear that the Fourier series representation for the equilibrium interaction potential $\phi_e(x,y)$, which was derived by means of reciprocal lattice formalism, is of the same form as the representation for an even function $F(x,y)$ with four fold symmetry and a mirror plane passing through the origin which was obtained by mathematical analysis. From a physical, as well as mathematical point of view, it is therefore justified to assume equation (2.51) as Fourier series representation for the equilibrium interaction potential above the substrate. Also, it has merit to put the details of the techniques on record.

2.6. Fourier series representation of the equilibrium height

In paragraph 2.5 the assumption is made that the equilibrium interaction potential $\phi_e(x,y)$ is a periodic function with the same periodicity and symmetry as the underlying substrate surface Bravais lattice. The same applies to the equilibrium height $z_{min}(x,y)$. The function $z_{min}(x,y)$ should also be invariant under all surface lattice translations [24], and have the same period and symmetry properties as $\phi_e(x,y)$. Thus it is justified to assume a Fourier series representation $H_{min}(x,y)$ for $z_{min}(x,y)$ which is of the same form as that of $\phi_e(x,y)$, viz.

$$H_{min}(x,y) = \frac{1}{4} B_{oo} + \frac{1}{2} \sum_{h=1}^{\infty} B_h[\cos 2\pi hx + \cos 2\pi hy]$$

$$+ \sum_{h,k=1}^{\infty} [B_{hk} \cos 2\pi hx \cos 2\pi ky] . \qquad (2.52)$$

All arguments concerning convergence, approximation by a partial sum and applicability of optimization methods pertaining to the equilibrium interaction potential $\phi_e(x,y)$, discussed in the next chapter also apply in the case of the equilibrium height z_{min}.

3. NUMERICAL PROCEDURE

3.1. Introduction

In this chapter the question of convergence of the two-dimensional Fourier series representation of the interaction potential, and the validity of a partial sum approximation containing a small number of terms is addressed. The applicability of the least squares and minimization methods to the present problem, as well as the details of the experimental methodology adopted in this study, will be discussed.

3.2. The truncated Fourier series representation

The ultimate goal of this study is to compute the coefficients for a two-dimensional Fourier series representation

$$F_e(x,y) = \frac{1}{4}A_{oo} + \frac{1}{2}\sum_{h=1}^{\infty} A_h[\cos 2\pi hx + \cos 2\pi hy] + \sum_{h,k=1}^{\infty} [A_{hk} \cos 2\pi hx \cos 2\pi ky] \qquad (3.1)$$

of the equilibrium interaction potential $\phi_e(x,y)$ of an argon atom on an argon crystal surface. However, in practice only a finite number of terms in this series can be computed. It is therefore important to know that the series in (3.1) does indeed converge, hopefully rapidly, to $\phi_e(x,y)$, so that partial sums of the series, containing a small number of terms, will give a good approximation to $\phi_e(x,y)$. According to Weinberger [41] the complete two-dimensional Fourier series converges absolutely and uniformly to $\phi_e(x,y)$ as a double series if $\phi_e(x,y)$ is

continuous and continuously differentiable, and if the squares of its second order partial derivatives have finite integrals. From a physical point of view we expect $\phi_e(x,y)$ to be a smooth continuous function satisfying the above mentioned *necessary* conditions, so that it can indeed be approximated by a partial sum

$$F_e(x,y) = \frac{1}{4}A_{oo} + \frac{1}{2}\sum_{h=1}^{N'} A_h[\cos 2\pi hx + \cos 2\pi hy]$$

$$+ \sum_{h,k=1}^{N'} A_{hk}[\cos 2\pi hx \cos 2\pi ky] \qquad (3.2)$$

to be referred to as a "truncated" Fourier series. The question concerning the number of terms needed in this partial sum in order to give a good approximation, will be discussed in a subsequent section. The Fourier coefficients have to be determined numerically as no simple analytical derivation of expressions for Fourier coefficients in two dimensions could be found. The method of least squares for fitting a chosen function to specific data is employed in the calculation of the Fourier coefficients.

3.3. The least squares method

This method can be used when the value of a function $Y(x)$, $x \in \mathfrak{A}^n$, is known at a finite number of points x_i, $i = 1,2, \ldots, M$, while the exact mathematical form of $Y(x)$ is unknown. By using the set of data points $\{(x_i,Y_i),\ i = 1,2, \ldots, M\}$, it is required to select a specific function f from a family of known functions such that the fit between Y and f is "best" in some sense [42].

In general it is assumed that f is of the form

$$f = f(\alpha_1, \alpha_2, \ldots, \alpha_k, x) = f(\underline{\alpha}, x), \tag{3.3}$$

where the k parameters $\alpha_1, \ldots, \alpha_k$ define the family of functions. It is now assumed that a "best" fit is obtained if the parameters, α_j, are selected so that:

$$\Delta^2 = \sum_{i=1}^{M} [Y_i - f(\alpha_1, \alpha_2, \ldots, \alpha_k, x_i)]^2 = \text{minimum}. \tag{3.4}$$

One way to achieve this is to require that

$$\frac{\partial \Delta^2}{\partial \alpha_j} = 0, \qquad j = 1,2, \ldots, k, \tag{3.5}$$

which yields k simultaneous equations. These equations have to be solved for the α_j, in order to determine a "best" or "least squares" approximate expression for the true function Y(x), with

$$Y(x) \doteq f(\alpha_1^*, \alpha_2^*, \ldots, \alpha_k^*, x), \tag{3.6}$$

where the superscript * pertains to the solution of equations (3.5).

The two-dimensional Fourier representation is now considered. For convenience $x \in \mathcal{R}^2$ is denoted by (x,y). In the present study the exact form of the equilibrium interaction potential $\phi_e(x,y)$ is the unknown function Y. For reasons of symmetry and other considerations which have been discussed above, it is assumed that $\phi_e(x,y)$ can be expressed as a two-dimensional truncated Fourier series of the form

$$F_e(\underset{\sim}{A}, x, y) = \frac{1}{4}A_{oo} + \frac{1}{2}\sum_{h=1}^{N'} A_h[\cos 2\pi hx + \cos 2\pi hy] + \sum_{h,k=1}^{N'} [A_{hk} \cos 2\pi hx \cos 2\pi ky]. \tag{3.7}$$

This series in unknown coefficients $\underset{\sim}{A} \equiv \{A_i\}$ now constitute the family of functions $f(\underline{\alpha},x)$.

For each grid point (x_i,y_j) a discrete value of the equilibrium interaction potential $\phi_e(x_i,y_j)$ is calculated using the relation:

$$\phi_e(x_i,y_j) = \sum_J^N 4\varepsilon[(\frac{\sigma}{R_{PJ}})^{12} - (\frac{\sigma}{R_{PJ}})^6] , \tag{3.8}$$

where

$$R_{PJ} = \sqrt{(x_i - x_J)^2 + (y_j - y_J)^2 + (z_{min}(x_i,y_j) - z_J)^2} \tag{3.9}$$

and the sum is taken over the finite number of atoms contained in the hemispherical part of the substrate with radius 5a and centre at (x_i,y_j) (See Fig. 2.3(a)). This is the calculated data to which the chosen form of the function $F_e(\underset{\sim}{A},x,y)$ (in the present study, the truncated Fourier series) is to be fitted by selecting the components of $\underset{\sim}{A}$ using the criterion

$$\Delta^2 = \sum_{i=1}^M [\phi_e^{Data}(x_i,y_j) - F_e(A_1, \ldots, A_K, x_i,y_j)]^2 = \text{minimum.} \tag{3.10}$$

In the present study a modified Levenburg-Marquardt algorithm is used to minimize the sum of squares. This method eliminates the need for explicit derivatives. In general the number, M, of data points will greatly exceed the number K of parameters (A_{oo}, A_h, A_{hk}).

3.4. The Golden Section search technique [43]

This method is a one-dimensional optimization direct search method which can be used when the position z^* of the minimum (or maximum) of a unimodal function f(z) of one independent variable z within a closed interval $a \leqslant z \leqslant b$ is to be determined. The technique comprises the following: The function of which the extremum is to be determined, is evaluated at a number of points. These data are used to estimate the approximate location of the desired extremum. The search is continued until the absolute difference in successive computed values of f is smaller than ε, where $\varepsilon > 0$ defines the desired accuracy.

From equations (2.8) and (2.10) it is clear that the interaction potential ϕ^P of a reference atom P will vary with its height z above the substrate, x and y being fixed. Accordingly ϕ^P is a function of only one independent variable z. Computing the sum over all the atoms in the hemispherical region of the substrate contributing to the potential at P, it is found, not surprisingly from a physical point of view, that ϕ^P is also a unimodal function (see Fig. 2.4) in the region of interest. Therefore the Golden Section search method can be applied to determine an approximate value for z_{min} and $\phi^P_{xy}(z_{min}) = \phi^P_e(x,y)$.

3.5. Methodology of the experiments

The suit of programmes developed to carry out the numerical computations proved to be surprisingly simple. It must however be noted that for the actual minimization two IMSL [44] subroutines ZXGSN and ZXSSQ were employed. ZXGSN is based on the Golden Section search technique, and ZXSSQ uses a modified Levenburg-Marquardt least squares

algorithm. (See appendices A and B).

A schematic representation of the numerical procedure followed in this study in the determination of the Fourier coefficients A_{hk} and B_{hk} and the height at which the equilibrium occurs, is presented below. Also indicated on the diagram is the method used to compute approximate values for $\phi_e(x,y)$ and $z_{min}(x,y)$ at any point (x,y) in the two-dimensional surface unit cell, using the computed Fourier coefficients.

In calculating the equilibrium interaction potential $\phi_e(x_i,y_j)$ at each mesh point (x_i,y_j), the interval in which the minimum of $\phi(x_i,y_j)$ is to be located is specified as

$0{,}095\,a \leqslant z \leqslant 2\,a$.

The length of the final subinterval containing the minimum is specified as $1{,}9 \times 10^{-8}$ a.

The convergence criteria of the subroutine ZXSSQ, which is used to minimize the sum of squares of the m^2 differences $[\phi_e(x_i,y_j) - F_e(\underset{\sim}{A},x_i,y_j)]$ and m^2 differences $[z_{min}(x_i,y_j) - H_{min}(\underset{\sim}{B},x_i,y_j)]$ respectively, at the m^2 data points, is manipulated in such a way that convergence be achieved only if on two successive iterations the parameter estimates $\underset{\sim}{A}$ and $\underset{\sim}{B}$ respectively, agree component by component to 7 significant digits. The values of the coefficients in the truncated Fourier series F_e and H_{min} have now been obtained. It is now possible to calculate values of F_e and H_{min} at any grid point (x,y) in the surface unit cell.

Flow Diagram of Numerical Procedure

1. Coordinates of substrate atoms which contribute towards the interaction potential are generated using eq. (2.7), and then stored.
2. Coordinates of grid points $\{(x_i,y_j)/i=1, \ldots m; j=1, \ldots m\}$ overlaying a two-dimensional unit cell with centre at the origin are generated.
3. For each grid point (x_i,y_j), $\phi_e(x_i,y_j) = \phi_{x_i,y_j}(z_{min})$ and z_{min} is determined using subroutine ZXGSN and eqs. (2.8) and (2.10).
4. x_i,y_j, $z_{min}(x_i,y_j)$ and $\phi_e(x_i,y_j)$ are stored for each point (x_i,y_j).

1. x_i,y_j and $\phi_e(x_i,y_j)$ are read for each grid point.
2. Subroutine ZXSSQ is used to minimize the sum of squares of the m^2 differences $[\phi_e(x_i,y_j) - F_e(\underset{\sim}{A}, x_i,y_j)]$ at the m^2 points in the mesh, where each $F_e(x_i,y_j)$ is a function of K variables (the Fourier coefficients A_{hk} which have to be determined).
3. The Fourier coefficients A_{hk} are stored.

1. The A_{hk} are read.
2. The coordinates of the grid point $\{(x_i,y_j)/i = 1, \ldots p; j = 1, \ldots p\}$ overlaying the two-dimensional unit cell with centre at the origin are generated.
3. $F_e(x_i,y_j)$ is calculated at each of the points (x_i,y_j), using equation (3.2) and the calculated values A_{hk}.
4. x_i, y_j, $F_e(x_i,y_j)$ for each point (x_i,y_j) are stored.

1. x_i,y_j and $z_{min}(x_i,y_j)$ are read for each grid point.
2. Subroutine ZXSSQ is used to minimize the sum of squares of the m^2 differences $[z_{min}(x_i,y_j) - H_{min}(\underset{\sim}{B}, x_i,y_j)]$ at the m^2 points in the mesh, where each $H_{min}(x_i,y_j)$ is a function of K variables (the Fourier coefficients B_{hk} which have to be determined).
3. The Fourier coefficients B_{hk} are stored.

1. The B_{hk} are read.
2. The coordinates of the grid point $\{(x_i,y_j)/i = 1, \ldots p; j = 1, \ldots p\}$ overlaying a two-dimensional unit cell with centre at the origin are generated.
3. $H_{min}(x_i,y_j)$ is calculated at each of the points (x_i,y_j), using an equation similar to (3.2) and the calculated values of B_{hk}.
4. x_i,y_j and $H_{min}(x_i,y_j)$ for each point (x_i,y_j) are stored.

4. NUMERICAL RESULTS AND DISCUSSION

4.1. Introduction

In this chapter the ability to calculate values of F_e and H_{min} at any grid point in the surface unit cell, is used to investigate the variations with position of ϕ_e and z_{min} accepting that F_e an H_{min} are adequate representations of ϕ_e and z_{min} respectively. F_e can also be utilised to calculate certain derived quantities like the desorption energy E_d of an adsorbed atom, the activation energy for surface migration E_a and the force constant k_τ^* for transverse (in xy-plane) atomic vibrations in positions of stable equilibrium, i.e. at the minima of the ϕ_e surface.

4.2. The Fourier coefficients A_{hk}

The specific form of the truncated Fourier series representation for the equilibrium interaction potential $\phi_e(x,y)$ used in the experiments is

$$F_e^n(x,y) = \frac{1}{4} A_{oo} + \frac{1}{4} \sum_{h=1}^{n} (A_{ho} + A_{oh})(\cos 2\pi hx + \cos 2\pi hy) + \sum_{h,k=1}^{n} A_{hk} \cos 2\pi hx \cos 2\pi ky \qquad (4.1)$$

where the truncation is after terms of order n. The order n of a Fourier coefficient A_{hk} is defined as h + k.

There are at least two factors that could influence the values of the calculated Fourier coefficients A_{hk}. The first is the number of data points (x_i, y_j) used in the calculations, and the second the order at which the series is truncated.

In the first series of experiments the number of data points is increased from 100 to 256, using $F_e^4(x,y)$. The results of these experiments are listed in Table 4.1.

TABLE 4.1.

Fourier coefficients A_{hk} obtained using 100, 144, 196 and 256 data points

Order	Number of data points	100	144	196	256
0	$A_{oo}/4$	-0,42310 D-01	-0,42310 D-01	-0,42310 D-01	-0,42310 D-01
1	$A_{o1}/4$	0,5893 D-02	0,5892 D-02	0,5892 D-02	0,5892 D-02
	$A_{1o}/4$	0,5893 D-02	0,5892 D-02	0,5892 D-02	0,5892 D-02
2	$A_{o2}/4$	-0,1217 D-02	-0,1216 D-02	-0,1216 D-02	-0,1216 D-02
	A_{11}	-0,1108 D-02	-0,1107 D-02	-0,1107 D-02	-0,1107 D-02
	$A_{2o}/4$	-0,1217 D-02	-0,1216 D-02	-0,1216 D-02	-0,1216 D-02
3	$A_{o3}/4$	0,310 D-03	0,307 D-03	0,307 D-03	0,307 D-03
	A_{12}	0,241 D-03	0,241 D-03	0,241 D-03	0,241 D-03
	A_{21}	0,241 D-03	0,241 D-03	0,241 D-03	0,241 D-03
	$A_{3o}/4$	0,310 D-03	0,307 D-03	0,307 D-03	0,307 D-03
4	$A_{o4}/4$	-0,94 D-04	-0,86 D-04	-0,86 D-04	-0,86 D-04
	A_{13}	-0,62 D-04	-0,62 D-04	-0,62 D-04	-0,62 D-04
	A_{22}	-0,48 D-04	-0,49 D-04	-0,49 D-04	-0,49 D-04
	A_{31}	-0,62 D-04	-0,62 D-04	-0,62 D-04	-0,62 D-04
	$A_{4o}/4$	-0,94 D-04	-0,86 D-04	-0,86 D-04	-0,86 D-04

We observe that the sign of the coefficients alternate with order and that $A_{hk} = A_{kh}$ which is consistent with the four fold symmetry of the model. To the specified accuracy of 7 significant digits, the calculated values for the

Fourier coefficients do not change as the number of data points are increased above 144. Thus 144 data points seem adequate both from point of view of accuracy, as well as economy in computer time.

The second series of experiments, where the order n of the truncation is increased from 3 to 6, is carried out using 144 data points. The results of this group of experiments are displayed in Table 4.2. From these results it follows that the inclusion of higher order harmonics does not alter the values of the lower order Fourier coefficients when working to an accuracy achievable by 7 significant digits.

The important question as to the rapidity at which the Fourier coefficients converge to zero with harmonic order, can now be considered. From the results displayed in Table 4.2. it follows numerically that the second order coefficients are approximately 4 to 5 times smaller than the first order coefficients, and that the third order coefficients are likewise about 4 times smaller than the second order ones. It is evident that the magnitude of the coefficients decreases rapidly with harmonic order. In fact, the magnitudes of the 5th order coefficients are only about 0,04% of those of the first order coefficients. This rapid convergence is what one could expect from such welbehaved functions as are displayed in Fig. 4.5.

Rieder and Stocker [45] investigated the interaction potential of the atoms with a{110} surface of Pd. They concluded from boundstate-resonance measurements that the ratio of the amplitude of the second and first order harmonic terms of the Fourier series is about 0,2.

TABLE 4.2

Fourier coefficients A_{hk} calculated for approximations truncated at the 3rd, 4th, 5th and 6th order terms respectively using 144 data points.

Order of truncation	Fourier coefficients	F_e^3	F_e^4	F_e^5	F_e^6
0	$A_{00}/4$	-0,42310 D-01	-0,42310 D-01	-0,42310 D-01	-0,42310 D-01
1	$A_{01}/4$	0,5892 D-02	0,5892 D-02	0,5892 D-02	0,5892 D-02
	$A_{10}/4$	0,5892 D-02	0,5892 D-02	0,5892 D-02	0,5892 D-02
2	$A_{02}/4$	-0,1216 D-02	-0,1216 D-02	-0,1216 D-02	-0,1216 F-02
	A_{11}	-0,1107 D-02	-0,1107 D-02	-0,1107 D-02	-0,1107 D-02
	$A_{20}/4$	-0,1216 D-02	-0,1216 D-02	-0,1216 D-02	-0,1216 D-02
3	$A_{03}/4$	0,307 D-03	0,307 D-03	0,307 D-03	0,307 D-03
	A_{12}	0,241 D-03	0,241 D-03	0,241 D-03	0,241 D-03
	A_{21}	0,241 D-03	0,241 D-03	0,241 D-03	0,241 D-03
	$A_{30}/4$	0,307 D-03	0,307 D-03	0,307 D-03	0,307 D-03
4	$A_{04}/4$		-0,86 D-04	-0,86 D-04	-0,86 D-04
	A_{13}		-0,62 D-04	-0,62 D-04	-0,62 D-04
	A_{22}		-0,49 D-04	-0,49 D-04	-0,49 D-04
	A_{31}		-0,62 D-04	-0,62 D-04	-0,62 D-04
	$A_{40}/4$		-0,86 D-04	-0,86 D-04	-0,86 D-04
5	$A_{05}/4$			0,28 D-04	0,28 D-04
	A_{14}			0,17 D-04	0,17 D-04
	A_{23}			0,11 D-04	0,11 D-04
	A_{32}			0,11 D-04	0,11 D-04
	A_{41}			0,17 D-04	0,17 D-04
	$A_{50}/4$			0,28 D-04	0,28 D-04
6	$A_{06}/4$				-0,8 D-05
	A_{15}				-0,5 D-05
	A_{24}				-0,2 D-05
	A_{33}				-0,1 D-05
	A_{42}				-0,2 D-05
	A_{51}				-0,5 D-05
	$A_{60}/4$				-0,8 D-05

This is in near agreement with the present results, if somewhat unexpected, because of the metallic substrate, but it is certainly encouraging!

4.3. A special case: The one-dimensional problem

For a one-dimensional Fourier approximation of a function of period 2π but with its values known at a discrete set of $2N+1$ equally spaced points in a period, analytical expressions for the Fourier coefficients were derived by Hildebrand [46]. The equilibrium interaction potential $\phi_e(x,0)$ along the x-axis is known to be an even function of period ℓ. According to Hildebrand

$$\phi_e(x,0) \approx G_H(x) = A_o + \sum_{k=1}^{n} (A_k \cos 2\pi kx + B_k \sin 2\pi kx), \qquad (4.2)$$

where $n \leqslant N$ and

$$A_o = \frac{1}{2N} \sum_{p=-N+1}^{N} \phi_e(x_p),$$

$$A_k = \frac{1}{N} \sum_{p=-N+1}^{N} \phi_e(x_p) \cos 2\pi kx_p, \qquad (k \neq 0,N) \qquad (4.3)$$

$$A_N = \frac{1}{2N} \sum_{p=-N+1}^{N} \phi_e(x_p) \cos 2\pi Nx_p,$$

$$B_k = \frac{1}{N} \sum_{p=-N+1}^{N} \phi_e(x_p) \sin 2\pi kx_p,$$

($B_k = 0$, because ϕ_e is an even function).

This reduces to

$$\phi_e(x,i) \approx G_H(x) = A_o + \sum_{k=1}^{n} A_k \cos 2\pi kx, \qquad (4.4)$$

where the coefficients are given by equations (4.3). The two-dimensional Fourier series representation to the order n for $\phi_e(x,y)$ used in this study is

$$F_e^n(x,y) = \frac{1}{4} A_{oo} + \frac{1}{4} \sum_{h=1}^{n} (A_{ho} + A_{oh})(\cos 2\pi hx + \cos 2\pi hy)$$

$$+ \sum_{h,k=1}^{n} A_{hk} \cos 2\pi hx \cos 2\pi ky \qquad (4.5)$$

Thus along the x-axis (with y=0 and k=0) one obtains the one-dimensional truncated Fourier representation

$$F_e^n(x,0) = \frac{1}{4} A_{oo} + \frac{1}{4} \sum_{h=1}^{n} (A_{ho} + A_{oh})(\cos 2\pi hx + 1) + \sum_{h=1}^{n} A_{ho} \cos 2\pi hx$$

$$= F_o + \sum_{h=1}^{n} F_h \cos 2\pi hx \qquad (4.6)$$

where

$$F_o = \frac{1}{4} A_{oo} + \frac{1}{2} \sum_{h=1}^{n} A_{ho} \quad \text{and} \quad F_h = \frac{3}{2} A_{ho} \qquad (4.7)$$

Clearly equations (4.4) and (4.6) are of the same form. Fourier coefficients A_k calculated using equations (4.3), as well as the corresponding coefficients F_h, calculated for the two-dimensional problem are displayed in Table 4.3.

Clearly there is and should be excellent agreement between the results obtained by the two methods. This strengthens our confidence in the present computed Fourier coefficients in two-dimensional representations.

TABLE 4.3

Coefficients calculated using Hildebrand's analytical expressions		Coefficients calculated using numerical least squares method	
A_o	-0,037393	F_o	-0,037393
A_1	0,004978	F_1	0,004976
A_2	-0,001015	F_2	-0,001011
A_3	0,000257	F_3	0,000255
A_4	-0,000077	F_4	-0,000071

4.4. Truncation of the Fourier series representation

The following important question may now be considered: At what order should a Fourier series be truncated in order that it still gives a good approximation of $\phi_e(x,y)$? The standard error [47], defined as

$$\delta = \sqrt{\sum_{i=1}^{p} \frac{[\phi_e(\bar{\tau}_i) - F_e^n(\bar{\tau}_i)]^2}{p}}, \qquad (4.8)$$

where the $\bar{\tau}_i$ are the position vectors of the grid points used in the calculation and p is the number of data points, should provide a good measure of the accuracy of the approximation $F_e^n(x,y)$. In the present study 49 data points in the first quadrant have been used (See Fig. 4.1).

The results of calculations of the standard error δ for F_e^1, F_e^2, F_e^3, F_e^4 and F_e^5 are depicted by means of the histogram in Fig. 4.2 where the primary computed values have been used for ϕ_e. It is evident that the standard error is greatly reduced if second order harmonics are also

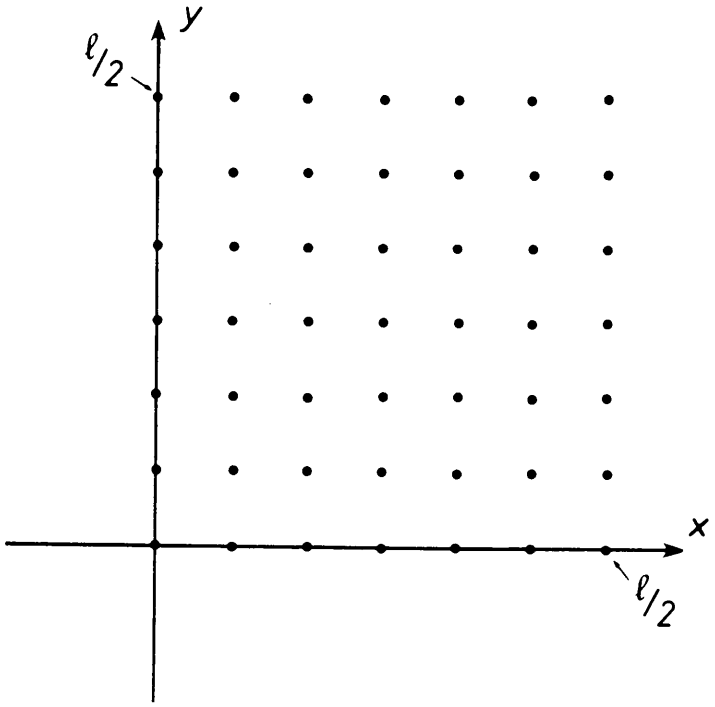

Fig. 4.1. First quadrant of unit cell showing the location of data points used in standard error calculations.

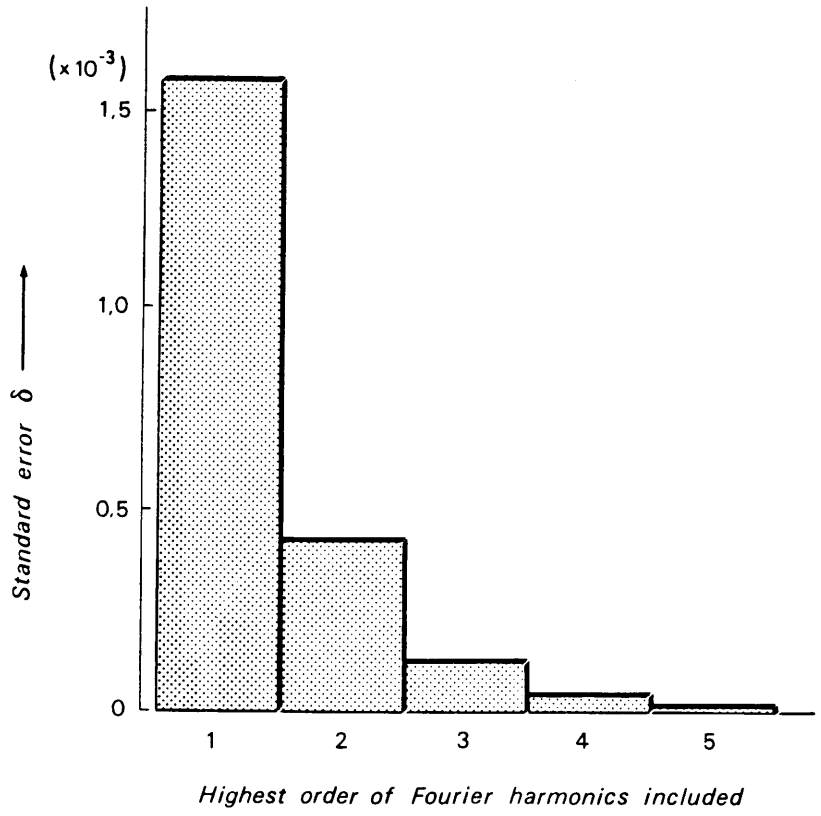

Fig. 4.2. Histogram illustrating the dependence of the standard error δ on the order of the truncation.

included in the approximation.

In Fig. 4.3 we show cross-sections through the potential energy surfaces at $y = 0$ as represented by $\phi_e(x,0)$, $F_e^1(x,0)$, $F_e^2(x,0)$ and $F_e^3(x,0)$ respectively. Curves for $F_e^4(x,0)$ and $F_e^5(x,0)$ are not shown since they are indistinguishable from $\phi_e(x,0)$. The figure illustrates how rapidly the Fourier series representation converges to $\phi_e(x,y)$ with increasing order of truncation.

If only first order terms are included in the approximation the standard error is as small as $1{,}56 \times 10^{-3}$ eV. This corresponds to a standard percentage error of less than 4%, where the standard percentage error $\delta_{\%}$ is defined as

$$\delta_{\%} = 100 \times \sqrt{\sum_{i=1}^{p} \{(\phi_e(\bar{\tau}_i) - F_e^1(\bar{\tau}_i)/\phi_e(\bar{\tau}_i)\}^2/p} \qquad (4.9)$$

The maximum percentage error in this case is about 10%.

On the basis of the evidence presented here F_e^5 is an excellent approximation to ϕ_e. However, when we use this in an analysis with the view of predicting the properties of adsorbed layers, for example, the mathematical complexity is formidable. From a physical point of view important properties of the relevant systems are largely determined by the symmetry only and perhaps whether a certain Fourier order is significant or not. The exact values of the Fourier coefficients are then useful but not essential. In such cases much physical information can be derived from series truncated after the first order. Naturally for an adequate description of physical phenomena all

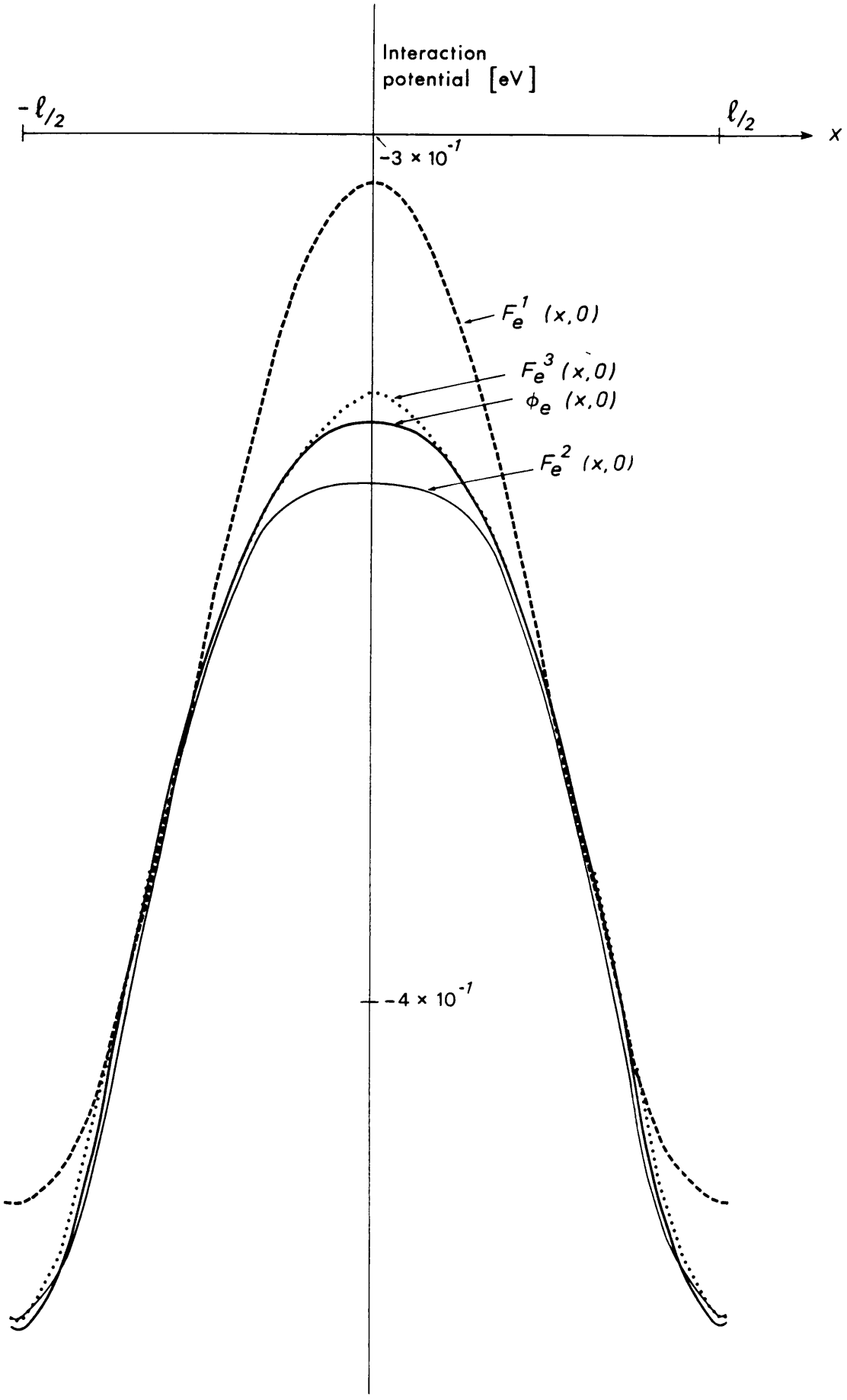

Fig. 4.3. Cross-sections through the potential energy surfaces as represented by $\phi_e(x,y)$, $F_e^1(x,y)$, $F_e^2(x,y)$ and $F_e^3(x,y)$ at $y = 0$.

significant terms must be included in the series. Reliable knowledge of Fourier coefficients will thus greatly improve the accuracy of models used in the description of a large category of physical phenomena.

4.5. Desorption and activation energy

In Fig. 4.5 intersections of a "vertical" plane (parallel to the x-axis) with the potential energy surface $F_e^5(x,y)$ through y=0, $\ell/4$ and $\ell/2$ are shown illustrating the variation of the potential energy with position in the unit cell. The three positions where the atom-solid interaction energy is of particular interest, are denoted by S, SP and A respectively in Fig. 4.4 [8].

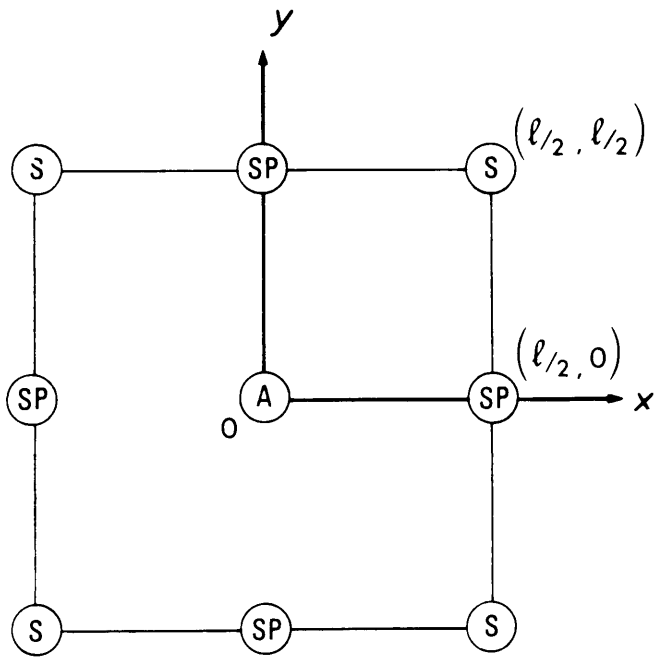

Fig. 4.4. Surface unit cell. The points denoted by A indicate the positions of the atoms in the surface plane of the substrate; adsorption sites are denoted by S; and saddle points in the potential function by SP.

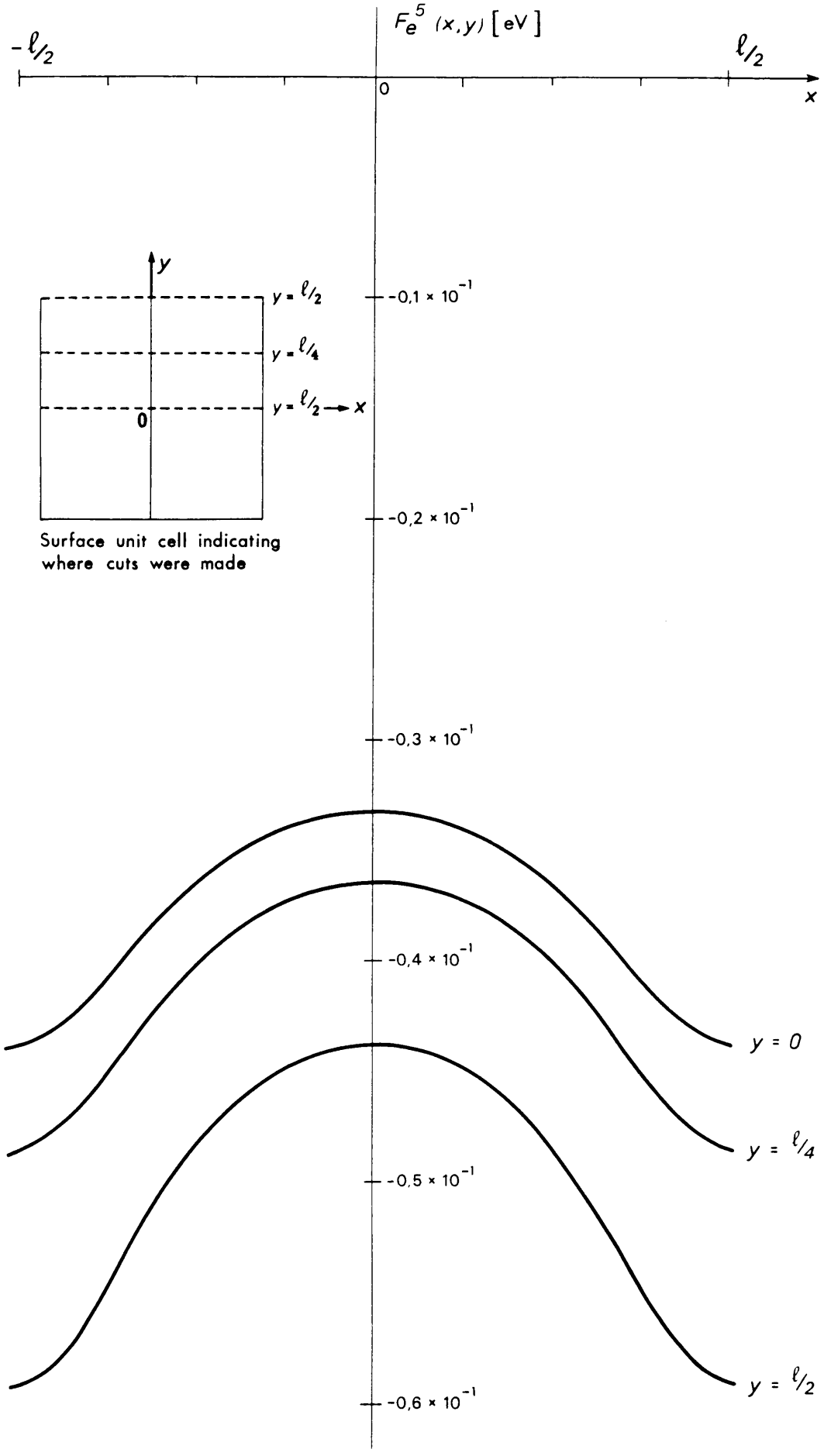

Fig. 4.5. Vertical cuts (parallel to the x-axis) through the potential energy surface $F_e^5(x,y)$ at $y = 0$, $\ell/4$ and $\ell/2$.

A corresponds to positions on top of a surface atom (maximum instability); SP to a saddle point and S to an adsorption site (minimum energy).

The desorption energy E_d of an adsorbed atom is the energy necessary to completely desorb it from a minimum energy position (adsorption site). Such a position is the point with coordinates $(\ell/2, \ell/2)$ in the two-dimensional unit cell, denoted by S in Fig. 4.4. The self-desorption energy of an argon atom can be read from the graph in Fig. 4.5 and is seen to be 0,0592 eV. (See Fig. 4.6).

The activation energy for surface migration of an atom is the potential barrier that an adsorbed atom must overcome to move from one preferred adsorption site to a neighbouring one. The points denoted by SP in Fig. 4.4 represent the minimum energy barriers that separate adsorption sites (denoted by S). The activation energy E_a for surface migration of an argon atom on an argon crystal surface can also be read from the graph in Fig. 4.5. This is the energy difference between the SP- and S-type point, i.e.

$$E_a = F_e^5(\ell/2,0) - F_e^5(\ell/2,\ell/2)$$

$$= 0,01546 \text{ eV}.$$

This may be confirmed with reference to Fig. 4.6.

Bacigalupi and Neustadter [7] used the Lennard-Jones (6-12) interaction potential to calculate the adsorption energy of an atom on the {100} plane of an fcc crystal substrate. From detailed topographical maps showing lines of equal adsorption energy, the maximum desorption energy and

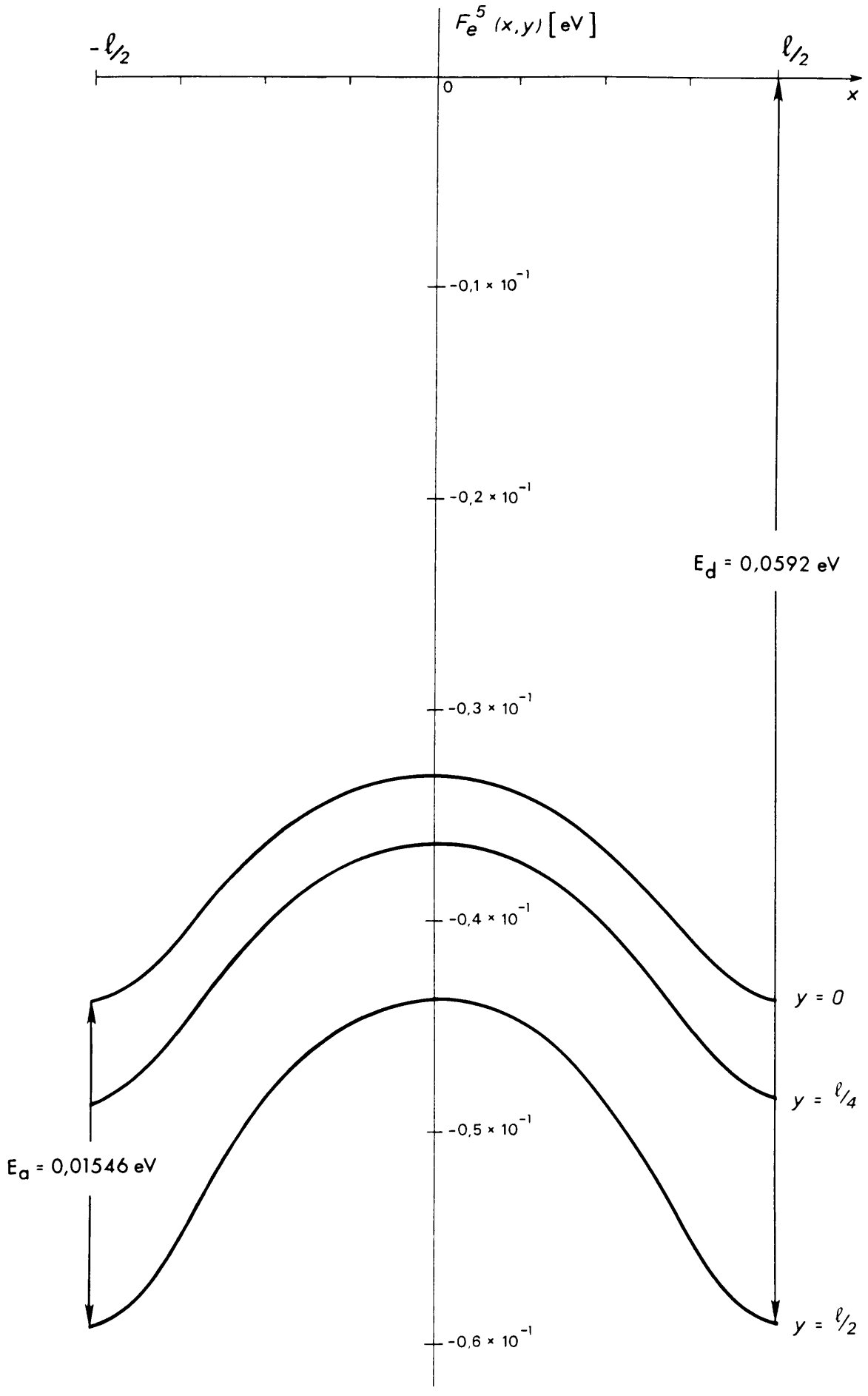

Fig. 4.6. Desorption energy E_d and activation energy for surface migration E_a for an argon atom on a {001} argon crystal surface.

minimum activation energy were determined for different ratios of σ/a. Their normalized values for these energies are listed in Table 4.3.

TABLE 4.3

Surface adsorption parameters for fcc {100} surface

$\sigma/a = 0.60$		$\sigma/a = 0.70$	
$E_d/4\varepsilon$	$E_a/4\varepsilon$	$E_d/4\varepsilon$	$E_a/4\varepsilon$
1,387	0,437	1,633	0,37

In the present study the value σ/a = 0,6587 was used. The normalised activation energy $E_a/4\varepsilon$ and the normalised desorption energy $E_d/4\varepsilon$ are found to be 0,395 and 1,513 respectively. These values are in agreement with the calculated values of Bacigalupi and Neustadter as should be expected. Also 4ε = 0,0391212 eV.

4.6. The lateral force constant k_{xy} for motion parallel to the surface

The two-dimensional Fourier series representation derived in this study can be utilised to compute a lateral force constant k_{xy}. Approximating the potential about the minimum by a two-dimensional harmonic oscillator model, k_{xy} is given by the second derivative of the potential function calculated at the minimum. Consider the following Fourier approximation of the potential in absolute coordinates.

$$F_e^3 = \frac{1}{4}A_{oo} + \frac{1}{2}\sum_{h=1}^{3} A_{ho}\cos(2\pi hx'/\ell) + \frac{1}{2}\sum_{h=1}^{3} A_{oh}\cos(2\pi hy'/\ell)$$

$$+ \sum_{h,k=1}^{h+k=3} [A_{hk}\cos(2\pi hx'/\ell)\cos(2\pi ky'/\ell)].$$

Hence

$$\frac{\partial^2 F_e^3}{\partial(x')^2} = -\frac{1}{2}(2\pi/\ell)^2 A_{10}\cos(2\pi x'/\ell) - \frac{1}{2}(4\pi/\ell)^2 A_{20}\cos(4\pi x'/\ell)$$

$$- (2\pi/\ell)^2 A_{11}\cos(2\pi y'/\ell)\cos(2\pi x'/\ell)$$

$$- \frac{1}{2}(6\pi/\ell)^2 A_{30}[\cos(6\pi x'/\ell)]$$

$$A_{12}[(2\pi/\ell)^2\cos(4\pi y'/\ell)\cos(2\pi x'/\ell)$$

$$+ (4\pi/\ell)^2\cos(2\pi y'/\ell)\cos(4\pi x'/\ell)].$$

The gas-solid energy is a minimum at point S (see figure 4.5) with coordinates $(\ell/2, \ell/2)$. The value of the force constant k_{xy} at point S is 0,0452554 eV/(Å)^2 which is equivalent to 525 °K/(Å)^2. However, the value of $k_{xy} = \partial^2 F_e/\partial(x')^2$ computed using a Fourier series approximation, is strongly dependent on the number of Fourier terms included in the approximation as can be seen from Table 4.4, where values of the force constant computed for approximations including first, second and third order Fourier terms respectively are listed. This is not surprising since our assumption of ignoring the variation in z, implicit in F_e, is probably not valid.

W.A. Steele [8] developed an analytic expression for pairwise additive gas-solid energies and utilised this expression to calculate minimum energies and lateral force constants for gas atoms on the (001) faces

TABLE 4.4

Values of the force constant calculated using approximations with increasing higher order of truncation.

Highest order terms included in Fourier approx. of potential	k_{xy} [eV/(Å)^2]	k_{xy} [°K/(Å)^2]
1	0,016814	195
2	0,033853	393
3	0,0452554	525

TABLE 4.5

Minimum energies and force constants for gas atoms on the (100) face of an fcc crystal [8].

$\sigma_{gs}/\underline{a}_1$	0,85	1,00
z_{min}/a_1	0,627	0,843
$\min \frac{u_s}{\varepsilon_{gs}}$	-5,500	-6,601
k_{xy}	2072	214

In the present study the following values were obtained for the corresponding quantities:

$$\sigma/\underline{a}_1 = 0,9316 ;$$

$$z_{min}/\underline{a}_1 = 0,7467 ;$$

$$\min F_e^3/\varepsilon = -6,135 ;$$

$$k_{xy} = 525.$$

of an fcc crystal. The values he obtained are listed in Table 4.5. This is in reasonable agreement with the findings of Steele.

4.7. Truncated Fourier series representation of the equilibrium height z_{min}

The specific form of the truncated Fourier series representation of z_{min} used in the calculations is

$$H^{n}_{min}(x,y) = \frac{1}{4} B_{oo} + \frac{1}{4} \sum_{h=1}^{n} (B_{ho} + B_{oh})(\cos 2\pi hx + \cos 2\pi hy) + \sum_{h,k=1}^{n} B_{hk} \cos 2\pi hx \cos 2\pi ky.$$

The computation of the B_{hk} procedes in the same manner as that of the A_{hk} as can be seen from paragraph 3.5.

A series of computer experiments is carried out, using 144 data points, to determine the effect of the inclusion of succesively higher order coefficients. The results are displayed in Table 4.6. We note that the constant term and the first order coefficients are positive. From the first to the fifth order the sign of the coefficients alternate with order. However, some sixth order coefficients are positive while others are negative. This is probably a consequence of limiting the calculations to 7 significant digits.

In Fig. 4.7 cross-sections are made through the equilibrium (height) surface $H^{6}_{min}(x,y)$ at $y = 0$, $y = \ell/4$ and $y = \ell/2$ respectively. The equilibrium height at a position directly above an atom in the surface plane of the substrate is 0,70379a. At an adsorption site the

TABLE 4.6

Order of coefficients		G_e^3	G_e^4	G_e^5	G_e^6
0	$B_{00}/4$	0,63449 D0	0,63449 D0	0,63449 D0	0,63449 D0
1	$B_{01}/4$	0,41279 D-01	0,41279 D-01	0,41279 D-01	0,41279 D-01
	$B_{10}/4$	0,41279 D-01	0,41279 D-01	0,41279 D-01	0,41279 D-01
2	$B_{02}/4$	-0,7142 D-02	-0,7142 D-02	-0,7142 D-02	-0,7142 D-02
	B_{11}	-0,3107 D-02	-0,3107 D-02	-0,3107 D-02	-0,3107 D-02
	$B_{20}/4$	-0,7142 D-02	-0,7142 D-02	-0,7142 D-02	-0,7142 D-02
3	$B_{03}/4$	0,1797 D-02	0,1797 D-02	0,1797 D-02	0,1797 D-02
	B_{12}	0,629 D-03	0,629 D-03	0,629 D-03	0,629 D-03
	B_{21}	0,629 D-03	0,629 D-03	0,629 D-03	0,629 D-03
	$B_{30}/4$	0,1797 D-02	0,1797 D-02	0,1797 D-02	0,1797 D-02
4	$B_{04}/4$		-0,492 D-03	-0,492 D-03	-0,492 D-03
	B_{13}		-0,144 D-03	-0,144 D-03	-0,144 D-03
	B_{22}		-0,99 D-04	-0,99 D-04	-0,99 D-04
	B_{31}		-0,144 D-03	-0,144 D-03	-0,144 D-03
	$B_{40}/4$		-0,492 D-03	-0,492 D-03	-0,492 D-03
5	$B_{05}/4$			0,162 D-03	0,162 D-03
	B_{14}			0,42 D-04	0,42 D-04
	B_{23}			0,0 D-06	0,0 D-06
	B_{32}			0,0 D-06	0,0 D-06
	B_{41}			0,42 D-04	0,42 D-04
	$B_{50}/4$			0,162 D-03	0,162 D-03
6	$B_{06}/4$				-0,73 D-04
	B_{15}				-0,13 D-04
	B_{24}				0,3 D-05
	B_{33}				-0,91 D-04
	B_{42}				0,3 D-05
	B_{51}				-0,13 D-04
	$B_{60}/4$				-0,73 D-04

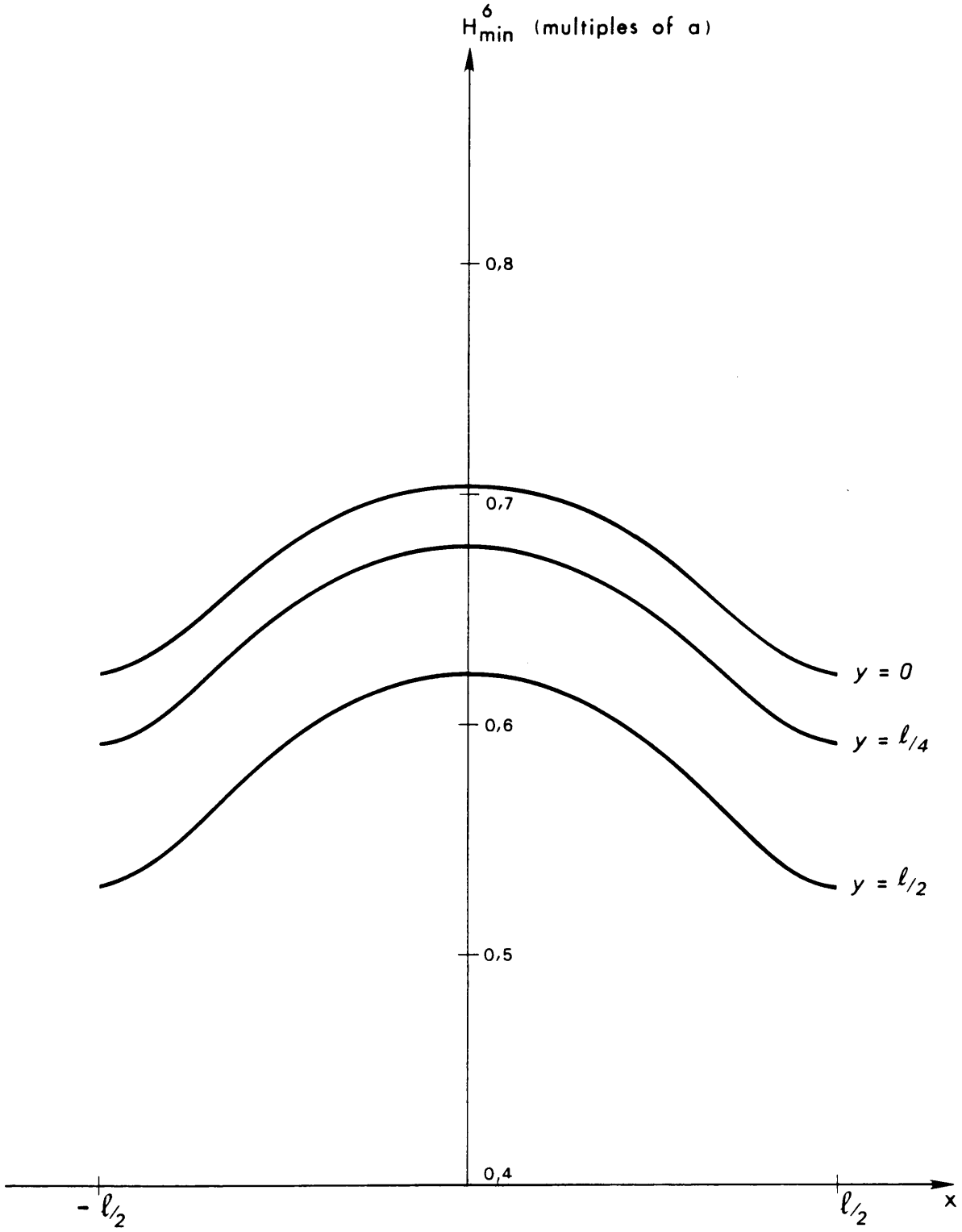

Fig. 4.7. Vertical cuts (parallel to the x-axis) through the equilibrium (height) surface $H^6_{min}(x,y)$ at $y = 0, \ell/4$ and $\ell/2$.

equilibrium height is 0,52815a. The value is slightly larger than the separation 0,5a of the (001) atomic planes. This deviation from the bulk lattice spacing thus exhibits an outward relaxation [48] of the (001) surface planes. This agrees with previous studies by L.C.A. Stoop [9].

4.8. Conclusions

The overall objectives of this study, namely to construct a Fourier series representation for the equilibrium interaction potential of an argon atom with a (001) argon crystal surface, as well as a Fourier series representation for the equilibrium height of a reference atom above the crystal substrate, have successfully been met. This was only possible and accomplished by the development of a *computational methodology* for calculating the numerical values of the Fourier coefficients in two-dimensional Fourier series representations. Having constructed the necessary tools, in the form of computer programs, it will now be comparatively easy to extend the work to more complicated systems involving for example other faces of fcc crystal substrates, as well as other lattice systems such as bcc and hcc.

Application of the computational technique to the special case of an argon atom on an argon crystal surface, illustrated to what extent important information can be derived from such a simple model. From computer experiments performed to investigate the influence on the numerical values of the Fourier coefficients when using Fourier approximations of the interaction potential truncated at increasing higher orders, it has been concluded that inclusion of higher order harmonics do not significantly alter the values of the lower order Fourier coefficients. The Fourier coefficients converged rapidly to zero with

harmonic order. This may not be true to the same extent for other systems. For more accurate approximations, increasingly higher order harmonics can easily be retained in the Fourier representation. (See eq. (4.1) and Table 4.2 for the relevant values of the coefficients). Indeed, we conclude that a series truncated after the fifth harmonic is an excellent approximation to the equilibrium interaction potential by any numerical standard.

From the fact that values for the coefficients in a one-dimensional representation obtained by putting $y = 0$ in the two-dimensional representation were verified using analytical expressions for the Fourier coefficients in a one-dimensional representation derived by Hildebrand [46], we concluded that our results may be viewed with confidence.

It was shown that satisfactory values of the desorption and activation energies of an adsorbed atom (compared to the work of Bacigalupi and Neustadter [7]), can be obtained using Fourier approximations truncated at low orders (see Fig. 4.3). It turned out that the lateral force constant k_{xy} for motion parallel to the surface is more sensitive to the truncation of the Fourier approximation. In order to obtain fair results when compared with calculations performed by Steele [8], at least third order harmonics must be included in the approximation. The sensitivity of the lateral force constant is probably due to the second order derivatives involved in its calculation.

The computed Fourier coefficients of the equilibrium height also converge to zero fairly rapidly with increasing order, although there is more variance in the magnitudes of the coefficients in a specific

order, particularly from the fifth and higher orders onwards. This may be partly due to numerical rounding errors. A slight outward relaxation of the (001) surface plane was observed as the equilibrium height at an adsorption site was 0,52815a as compared to the distance of 0,5a between substrate layers. This agrees with previous work by L.C.A. Stoop [9].

The possibilities of the present numerical model are by no means exhausted. It is planned to extend this work to calculations of the vertical force constant, as well as the contribution of different substrate atom layers towards the equilibrium interaction potential at the surface.

Although the present study was only concerned with the computation of a Fourier series representation for the equilibrium interaction potential at the (001) face of an fcc crystal, its real impact lies in the fact that a *numerical technique* for the calculation of Fourier coefficients in two-dimensional Fourier series representations, implicitely also incorporating the third dimension, has been developed and proven. It is the intention to extend this technique to calculate the interaction potential at a wide selection of faces for several crystal structures, using more realistic interatomic potentials, possibly including the effects of many-body forces and zero-point kinetic energy. The outcome of such calculations will contribute greatly towards our understanding of surface phenomena.

APPENDIX A

Algorithm

ZXGSN computes to the desired accuracy, the independent variable value that minimizes a unimodal function of one independent variable, where a known finite interval contains the minimum, using the Golden Section search technique.

Graphically, the function to be minimized is of the following form.

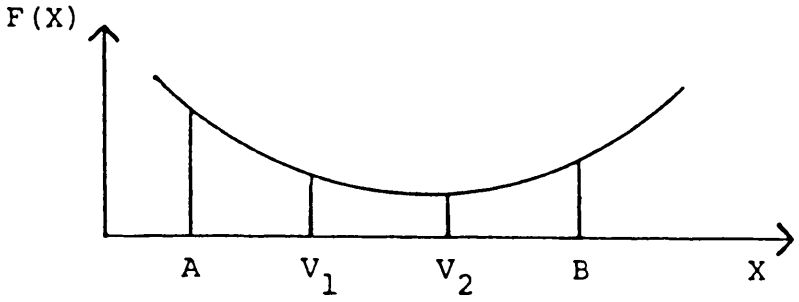

The number of iterations required to compute the minimizing value to accuracy TOL is the greatest integer less than or equal to

$$\left[\frac{\ln\left(\frac{TOL}{B-A}\right)}{\ln(1-C)}\right]+1$$

and $C = (3-\sqrt{5})/2$.

The first two test points are V_1 and V_2, are defined to be

$V_1 = A + C * (B-A)$

$V_2 = B - C * (B-A)$

where $C = (3-\sqrt{5})/2$

If $F(V_1)$ is less than $F(V_2)$, the minimizing value is in (A,V_2). In this case B is set to V_2, V_2 becomes the new V_1 and V_1 becomes $A+C*(B-A)$. If $F(V_1)$ is greater than or equal to $F(V_2)$, the minimizing value is in (V_1,B). In this case A is set to V_1, V_1 is set to V_2 and V_2 becomes $B-C*(B-A)$.

The algorithm continues in an analogous manner where only one new test point is computed at each step.

This process continues until the desired accuracy, TOL, is achieved. XMIN is set to the point producing the minimum value for the current iteration.

Athough, mathematically, the algorithm always produces the minimizing value to the desired accuracy, numerical problems may be encountered. If F is "too flat" in part of the region of interest, the function may appear constant to the computer in that region. Terminal error 131 indicates that this problem has occurred. The user may rectify the problem by relaxing the requirement on TOL, modifying (scaling, etc.) the form of F, or executing the program in a higher precision.

See references:

1. Brent, Richard P., Algorithms for Minimization Without Derivatives, Prentice-Hall, Inc., Englewood Cliffs, 1973, Chapter 5.

2. Hausman, Jr., R. F., "Function optimization on a line segment by Golden Section", Lawrence Radiation Laboratory, University of California-Livermore, April, 1971.

3. Spang, III, H. A., "A review of minimization techniques for non-linear functions", SIAM Review, 4(4)1962, 357-359.

APPENDIX B

Algorithm

ZXSSQ is a finite difference, Levenberg-Marquardt routine for solving nonlinear least squares problems. The problem is stated as follows:

given M nonlinear functions $f_1, f_2, \ldots, f_M$ of a vector parameter $\underset{\sim}{x}$,

minimize $f_1(\underset{\sim}{x})^2 + f_2(\underset{\sim}{x})^2 + \ldots + f_M(\underset{\sim}{x})^2$ over $\underset{\sim}{x}$

where $\underset{\sim}{x} = (x_1, x_2, \ldots, x_N)$ is a vector of N parameters to be estimated.

When fitting a nonlinear model to data, the functions f_i should be defined as follows:

$$f_i(\underset{\sim}{x}) = y_i - g(\underset{\sim}{x}; \underset{\sim}{v}^i) \qquad i=1,2,\ldots,M \quad \text{(i.e., the residuals)}$$

where y_i is the i-th observation of the dependent variable,

$\underset{\sim}{v}^i = (v_1^i, v_2^i, \ldots, v_{NV}^i)$ is a vector containing the i-th observation of the NV independent variables, and

g is the function defining the nonlinear model.

ZXSSQ is based on a modification of the Levenberg-Marquardt algorithm which eliminates the need for explicit derivatives.

Let $\underset{\sim}{x}^0$ be an initial estimate of $\underset{\sim}{x}$. A sequence of approximations to the minimum point is generated by

$$\underset{\sim}{x}^{n+1} = \underset{\sim}{x}^n - [\alpha_n D_n + J_n^T J_n]^{-1} J_n^T \underset{\sim}{f}(\underset{\sim}{x}^n),$$

where J_n is the numerical Jacobian matrix evaluated at $\underset{\sim}{x}^n$

D_n is a diagonal matrix equal to the diagonal of $J_n^T J_n$ for IOPT≠0.

α_n is a positive scaling constant (Marquardt parameter)

When forward differences are used, the Jacobian is calculated by

$$\frac{1}{h_j}[f_i(\underset{\sim}{x}+h_j\underset{\sim}{u}_j) - f_i(\underset{\sim}{x})]$$

where $\underset{\sim}{u}_j$ is the j-th unit vector and $h_j = \max(|x_j|, 0.1) \cdot eps^{1/2}$ (see scaling comments in Programming Note 2), where eps is the relative precision of floating point arithmetic. For central differences

$$\frac{1}{2h_j}\,[f_i(\underset{\sim}{x}+h_j\underset{\sim}{u}_j) - f_i(\underset{\sim}{x}-h_j\underset{\sim}{u}_j)]$$

is used. To minimize the number of function evaluations required for nonzero IOPT, a rank one update to the Jacobian matrix is used where appropriate:

$$J_{n+1} = J_n + \frac{1}{\underset{\sim}{\delta}^T\underset{\sim}{\delta}}\,[\underset{\sim}{f}(\underset{\sim}{x}^{n+1})-\underset{\sim}{f}(\underset{\sim}{x}^{n})-J_n\underset{\sim}{\delta}]\,\underset{\sim}{\delta}^T$$

where $\underset{\sim}{\delta} = \underset{\sim}{x}^{n+1} - \underset{\sim}{x}^{n}$.

See references:

1. Brown, K. M., and Dennis, J. E., "Derivative free analogues of the Levenberg-Marquardt and Gauss algorithms for nonlinear least squares approximations", Numerische Mathematik, 18, 1972, 289-297.

2. Brown, K. M., "Computer oriented methods for fitting tabular data in the linear and nonlinear least squares sense", Department of Computer, Information, and Control Sciences, TR No. 72-13, University of Minnesota.

3. Levenberg, K., "A method for the solution of certain non-linear problems in least squares", Quart. Appl. Math., 2, 1944, 164-168.

4. Marquardt, D. W., "An algorithm for least-squares estimation of nonlinear parameters", J. SIAM, 11(2)1963.

REFERENCES

[1] G. Binnig, H. Rohrer, Scientific American 253 (no 2), 40 (1985).

[2] R.M. Tromp, R.J. Hamers, and J.E. Demuth, Phys. Rev. Lett. 55, 1303 (1985).

[3] M. Mostoller and M. Rasolt, Phys. Lett. 88A, 93 (1982).

[4] C.A. Morrison, R.P. Leavitt, D.E. Wortman and N. Karayianis, Surface Sci. 62, 397 (1977).

[5] J.D. Weeks and G.H. Gilmer, J. Crystal Growth 33, 21 (1976).

[6] J.Q. Broughton and G.H. Gilmer, Acta metall. 31, 845 (1983).

[7] R.J. Bacigalupi and H.E. Neustadter, Surface Sci. 19, 396 (1970).

[8] W.A. Steele, Surface Sci. 36, 317 (1973).

[9] L.C.A. Stoop, Thin Solid Films 42, 33 (1977).

[10] J.Q. Broughton and G.H. Gilmer, J. Chem. Phys. 79, 5095 (1983).

[11] J.Q. Broughton and G.H. Gilmer, J. Chem. Phys. 79, 5105 (1983).

[12] J.Q. Broughton and G.H. Gilmer, J. Chem. Phys. 79, 5119 (1983).

[13] L.C.A. Stoop, Thin Solid Films 103, 375 (1983).

[14] J.A. Snyman and H.C. Snyman, Surface Sci. 105, 357 (1981).

[15] L.W. Bruch and J.A. Venables, Surface Sci. 148, 167 (1984).

[16] J.W. Matthews, *Epitaxial Growth* (Academic Press, New York, 1975).

[17] J.H. van der Merwe, Phil. Mag. A45, 127, 145, 159 (1982).

[18] N.W. Ashcroft and N.D. Mermin, *Solid State Physics* (Saunders College, Philadelphia, 1981) p 398.

[19] N.W. Ashcroft and N.D. Mermin, *Solid State Physics* (Saunders College, Philadelphia, 1981) p 390.

[20] N.W. Ashcroft and N.D. Mermin, *Solid State Physics* (Saunders College, Philadelphia, 1981) p 412.

[21] N.W. Ashcroft and N.D. Mermin, *Solid State Physics* (Saunders College, Philadelphia, 1981) p 399.

[22] C. Kittel, *Introduction to Solid State Physics* (Wiley, New York, 1971) p 102.

[23] C. Kittel, *Introduction to Solid State Physics* (Wiley, New York, 1971) p 105.

[24] C. Kittel, *Introduction to Solid State Physics* (Wiley, New York, 1971) p 63.

[25] M. Born and J.E. Mayer, Z. Physik 75, 1 (1932).

[26] J.E. Lennard-Jones, Proc. Roy. Soc. 43, 461 (1931).

[27] E.M. Chan, M.J. Buckingham and J.L. Robins, Surface Sci. 67, 285 (1977).

[28] N. Bernardes, Phys. Rev. 112, 1534 (1958).

[29] J.A. Barker, R.A. Fisher and R.O. Watts, Mol. Phys. 4, 657 (1971).

[30] M.B. Doran and I.J. Zucker, J. Phys. C4, 307 (1971).

[31] J.A. Barker, C.H.J. Johnson and T.H. Spurling, Austral. J. Chem. 25, 1811 (1972).

[32] J.A. Barker and A. Pompe, Aust. J. Chem. 21, 1683 (1968).

[33] D. Levesque and J. Vieillard Baron, Physica 44, 345 (1969).

[34] L. Verlet, Phys. Rev. 159, 98 (1967).

[35] D. Nicholson, Surface Sci. 151, 553 (1985).

[36] F.M. Mourits and F.H.A. Rummens, Can. J. Chem. 55, 3007 (1977).

[37] W.A. Steele, *The Interaction of Gases with Solid Surfaces* (Pergamon Press, New York, 1974) p 13.

[38] F. Jona, J. Phys. C 11, 4271 (1978)

[39] R.A. Johnson, Phys. Rev. B 27, 3861 (1983).

[40] H.F. Weinberger, *A First Course in Partial Differential Equations* (Wiley, New York, 1965) pp 141 - 142.

[41] H.F. Weinberger, *A First Course in Partial Differential Equations* (Wiley, New York, 1965) pp 143 - 145.

[42] R.E. Collins, *Mathematical Methods for Physicists and Engineers* (Reinhold, New York, 1968) p 360.

[43] B.S. Gottfried and J. Weisman, *Introduction to Optimization Theory* (Prentice-Hall, New Jersey, 1973) pp 68 - 83.

[44] IMSL, NBC Building, 7500 Bellaire Boulevard, Houston, Texas, U.S.A.

[45] K.H. Rieder and W. Stocker, J. Phys. C 16, L 783 (1983).

[46] F.B. Hildebrand, *Introduction to Numerical Analysis* (McGraw-Hill, New York, 1956) pp 373 - 376.

[47] J.F. Kenney and E. S. Keeping, *Mathematics of Statistics, Part One* (Van Nostrand, New Jersey, 1954) p 187.

[48] M. Prutton, *Surface Physics* (Oxford University Press, London, 1975) pp 2 - 3.